Predicting Efficient Antenna Ligands for Tb(III) Emission

Amanda P. S. Samuel,[†‡] Jide Xu,[†] Kenneth N. Raymond[†‡]*

Contribution from the Department of Chemistry, University of California, Berkeley, CA 94720-1460

raymond@socrates.berkeley.edu

RECEIVED DATE (to be automatically inserted after your manuscript is accepted if required according to the journal that you are submitting your paper to)

TITLE RUNNING HEAD: Predicting Efficient Antenna Ligands for Tb(III) Emission

CORRESPONDING AUTHOR FOOTNOTE:

[†]University of California, Berkeley

[‡]Lawrence Berkeley National Laboratory

ABSTRACT: A series of highly luminescent Tb(III) complexes of para-substituted 2-hydroxyisophthalamide ligands (5LI-IAM-X) has been prepared (X = H, CH_3, $(C=O)NHCH_3$, SO_3^-, NO_2, OCH_3, F, Cl, Br) to probe the effect of substituting the isophthalamide ring on ligand and Tb(III) emission in order to establish a method for predicting the effects of chromophore modification on Tb(III) luminescence. The energies of the ligand singlet and triplet excited states are found to increase linearly with the π-withdrawing ability of the substituent. The experimental results are supported by

time-dependent density functional theory (TD-DFT) calculations performed on model systems, which predict ligand singlet and triplet energies within ~5% of the experimental values. The quantum yield (Φ) values of the Tb(III) complex increases with the triplet energy of the ligand, which is in part due to the decreased non-radiative deactivation caused by thermal repopulation of the triplet. Together, the experimental and theoretical results serve as a predictive tool that can be used to guide the synthesis of ligands used to sensitize lanthanide luminescence.

KEYWORDS: Terbium; Luminescence; Antenna Effect; Triplet excited state energy; Coordination chemistry; Hammett parameter; TD-DFT.

Introduction

The high sensitivity and ease of detection afforded by fluorescent labels has made use of fluorescence-based bioassays very widespread. A wide variety of luminescent reporters such as organic fluorophores,[1,2] fluorescent proteins,[3,4] and fluorescent metal complexes[5,6] and nanoparticles,[7-9] have been incorporated into such systems. Among these, strategies based on lanthanide luminescence offer distinct advantages due to the unique photophysical properties (up to ms lifetimes, large Stokes shifts, narrow emission lines) of Ln(III) complexes. In particular, time-resolved luminescence-based assays utilize the long lifetimes of lanthanide complexes to increase detection sensitivity by eliminating the short-lived background fluorescence of biological samples.[10]

The luminescence of Ln(III) ions results from Laporte-forbidden *f-f* transitions, which give rise to their micro- to millisecond fluorescence lifetimes. However, because they are forbidden, these transitions exhibit low extinction coefficients ($\varepsilon < 1$ M^{-1}cm^{-1}).[11] The weak absorbance can be overcome by coordinating chromophore-containing ligands to the metal ion, which, upon irradiation, transfer

2

energy to the metal center, typically *via* the ligand triplet excited state, populating the Ln(III) emitting levels in a process known as the antenna effect.[11] The overall quantum yield (Φ) for a sensitized Ln(III) complex is given by the equation: $\Phi = \eta_{ISC}\eta_{ET}\Phi^{Ln}$; where η_{ISC} and η_{ET} are the respective efficiencies of intersystem crossing (ISC) and ligand-to-Ln(III) energy transfer, and Φ^{Ln} is the intrinsic quantum yield of the Ln(III) ion. In terms of ligand design, this means that the antenna chromophore should: (i) be efficient at absorbing light (i.e. have large ε values), (ii) have an ISC quantum yield near unity (iii) have a triplet state that is close enough in energy to the Ln(III) emitting state to allow for effective ligand-to-Ln(III) energy transfer (but not so close that thermal back-transfer competes effectively with Ln(III) emission) (iv) protect the Ln(III) from the quenching effects of bound water molecules. For practical use in biological applications, the ligands should also form Ln(III) complexes that are water-soluble and thermodynamically and kinetically stable.

A wide array of antenna chromophores that yield emissive Ln(III) complexes have been studied extensively, including bipyridines,[11-14] calixarenes,[15-17] and dipicolinic acids,[18,19] to highlight a few. In addition, computational studies of antenna ligands and metal complexes have provided significant insight into the energy transfer process.[20,21] Despite these advances, it remains difficult to easily and reliably predict the absorption and emission properties of new antenna ligands and Ln(III) complexes, without employing costly and time-consuming computational methods. The development of a simple and accurate model that can be used to screen potential antenna chromophores would represent an important advancement in the field of ligand-sensitized lanthanide luminescence.

Our previous work has shown that the 2-hydroxyisophthalamide (IAM) chromophore is an exceptionally good sensitizer of the visible Ln(III) emitters (Sm(III), Eu(III), Tb(III) and Dy(III)) while providing stable, water-soluble complexes.[22-24] The IAM-based Tb(III) complexes display some of the highest quantum yield values reported in the literature of Ln(III) complexes in aqueous solution at physiological pH.[22] Because of their remarkable brightness, these complexes have been incorporated as

fluorophores in commercial high-sensitivity assays.[25]   Using the IAM chromophore, we sought to develop a predictive tool that can be used to guide antenna ligand synthesis by studying a family of modified IAMs and their Ln(III) complexes. To this end, a series of para-substituted IAMs (5LI-IAM-X; X = H, CH$_3$, (C=O)NHCH$_3$, SO$_3^-$, NO$_2$, OCH$_3$, F, Cl, Br) (Figure 1) was synthesized. The addition of substituents to an antenna chromophore is commonly employed to alter the ligand energy levels and therefore modulate ligand-to-Ln(III) energy transfer.[12,16,18,19,26-34]   These tetradentate IAM ligands, which form eight-coordinate 2:1 ligand:Ln(III) complexes, serve as simplified analogs of the previously reported octa- and hexadentate ligands. The substituents cover a broad range of electron-donation and – withdrawing abilities that alter singlet and triplet energies and therefore tune the ligand energy levels to optimize energy transfer to the lanthanide ion. The photophysical measurements of the 5LI-IAM-X ligands and the Tb-5LI-IAM-X complexes are reported here along with computational studies of ligand excited state energies, which together form the basis for prediction of antenna ligand and Ln(III) complex properties.

Results and Discussion

Synthesis. The nine 5LI-IAM-X ligands were synthesized according to the procedures shown in Scheme 1.   To synthesize the chloro- and bromo-substituted ligands, the corresponding 2,6-dimethylphenols (**1a-b**) were first methyl-protected using dimethyl sulfate (DMS).   These dimethyl anisole derivatives (**2a-b**) were then oxidized with KMnO$_4$ to give the methoxyisophthalic acids (**6a-b**). To synthesize the fluoro- and methoxy-substituted ligands, the substituted phenols (**3c-d**) were treated with formaldehyde in basic media to give the bis-hydroxymethylated species (**4c-d**). The phenolic oxygens of the bis-hydroxymethyl phenols were benzyl-protected with benzyl chloride to give **5c** and **5d** after which the hydroxymethyl groups were oxidized using Jones reagent[35]   to afford the benzyloxyisophthalic acids (**6c-d**).   The methyl-substituted ligand was synthesized from 2,6-

4

bis(hydroxymethyl)-p-cresol (**4e**), which was methyl-protected using DMS to give **5e**. This compound was then oxidized to the acid (**6e**) with KMnO$_4$. The nitro-substituted methoxyisophthalic acid (**6g**) was prepared by nitrating the unsubstituted acid[36] (**6f**) with a 1:2 mixture of HNO$_3$:H$_2$SO$_4$. The para-substituted methoxyisophthalic acids (**6**) were converted to the activated bis-thiazolide species (**7**). The bifunctionalized thiazolides were selectively coupled with methylamine under high-dilution conditions to give the mono-methylamides (**8**). These methylamides were then coupled to the 1,5-diaminopentane backbone to give the protected ligands (**9**). The methyl protecting groups were removed using BBr$_3$ while the benzyl protecting groups were removed by hydrogenation or under strongly acidic conditions. The sulfonated ligand (**10i**) was prepared by sulfonation of the unsubstituted ligand (**10f**) using H$_2$SO$_4$.

The Ln(III) complexes were synthesized by combining two equivalents of ligand with one equivalent of LnCl$_3$•nH$_2$O in the presence of an excess of base (*sym*-collidine or pyridine) in methanol. After heating for several hours, the complexes were recrystallized from diethyl ether. The presence of the ML$_2$ complex for each of the compounds was confirmed by mass spectrometry (ES-) and elemental analysis. The Tb(III) complexes, prepared *in situ* by combining 1 equivalent of TbCl$_3$ (in 1M HCl) with 2 equivalents of ligand (in DMSO) in 0.1 M Tris buffered H$_2$O (pH = 7.4), displayed photophysical properties identical to the corresponding isolated Tb(III) complexes and therefore were used in this study to measure quantum yield and lifetime values.

Absorption and Emission. Photophysical measurements of the Ln(III) complexes of the 5LI-IAM-X series were performed to determine how the substituents affect the ligand excited states and Ln(III) emission. A summary of the results for the entire series is given in Table 1. The Tb(III) complexes (**Tb-X**) are very efficient absorbers, with extinction coefficients on the order of 2.3×10^4 M^{-1}cm^{-1}. Notably, this value for **Tb-NO$_2$** is twice as large as those of the other complexes, suggesting that this ligand experiences a larger change in dipole moment upon going from the ground to the excited state than do the other ligands.[37] The Tb(III) complexes, in aqueous solution, display single ligand-centered

absorption bands, as shown in Figure 2 in the representative absorption and emission spectra of **Tb-Cl**, with the exception of **Tb-Amide**, which shows one absorption band at 335 nm and a more intense band at 280 nm (Figure S2) and **Tb-NO$_2$**, which also displays two bands, one centered at 346 nm, and a shoulder at ~380 nm (Figure S8). The absorption maximum of the Tb(III) complex of the unsubstituted ligand (**Tb-H**) appears at 335 nm (Figure S1), which is consistent with the corresponding values observed for unsubstituted octadentate IAM ligands in aqueous solution.[22,24] The absorption maxima of the remaining complexes are red-shifted, ranging from 340 nm for **Tb-SO$_3^-$** to 359 nm **Tb-OCH$_3$** (Figures S3-S8). Residual ligand-centered fluorescence, which can be seen in the emission spectra of the Tb(III) complexes, covers a similarly broad range of energies. The unsubstituted ligand (**5LI-IAM-H**) has a fluorescence maximum of 408 nm, while the amide and sulfonate-substituted ligands fluoresce at slightly higher energies (405 and 404 nm, respectively). Fluorescence maxima for the other series members are red-shifted and range from 424 nm (**5LI-IAM-CH$_3$**) down to 450 nm (**5LI-IAM-OCH$_3$**), as can be seen in Figure 2 for **Tb-Cl** (**10a**) (see also Figures S1-S8).

To determine the ligand triplet excited state energies, the emission spectra of their respective Gd(III) complexes were recorded at 77K (Figures S9-S17). The lowest-energy emitting state of Gd(III), at 32,150 cm^{-1}, is too high to be excited by the antenna ligands used in this study. Consequently, emission spectra of the Gd(III) complexes show exclusively ligand-centered emission.[38] The emission spectra were de-convoluted to determine the 0-0 vibrational transition energy (T$_{0-0}$). The T$_{0-0}$ state of the unsubstituted ligand (**5LI-IAM-H**), at 23,330 cm^{-1} (429 nm), is ~3,000 cm^{-1} higher in energy than the emitting $^5D_4$ transition of Tb(III) (20,400 cm^{-1}), and is therefore in the range proposed for optimal ligand-to-Tb(III) energy transfer.[24] The amide and -SO$_3^-$ substituents result in higher energy T$_{0-0}$ states: 23,970 cm^{-1} (417 nm) and 23,870 cm^{-1} (419 nm), respectively. The T$_{0-0}$ states of the remaining ligands are red-shifted relative to **5LI-IAM-H** with **5LI-IAM-NO$_2$** and **5LI-IAM-OCH$_3$** having the lowest energy T$_{0-0}$ states, at 21,410 cm^{-1} (467 nm) and 19,860 cm^{-1} (504 nm), respectively. The **5LI-IAM-**

OCH₃ triplet state is more than 500 cm^{-1} below the $^5D_4$ emitting state and is therefore not expected to sensitize Tb(III) emission at room temperature.[31]

The Hammett substituent parameters,[39] σ_p, and the inductive/field ($\boldsymbol{F}$) and resonance ($\boldsymbol{R}$) component parameters were examined to see if they correlated with the absorption and emission energies of the IAM chromophores. Such a correlation would provide a preliminary strategy for IAM-ligand design. No correlation was observed between the σ_p parameters and the absorption and emission energies; however linear relationships were seen between the resonance component of the Hammett parameters, $\boldsymbol{R}$, and the ligand absorption and emission data. This indicates that the substituent's main influence is *via* interaction with π-system of the chromophore. Similar correlations have been observed for other comparable *para*-substitued chromophores, such as diphenylboron-2(pyrazolyl)aniline chelates.[40] The absorption, fluorescence, and phosphorescence energies of the **5LI-IAM-X** ligands all increase linearly with the π-withdrawing ability of the substituents (*i.e.*, with increasing $\boldsymbol{R}$ values) (Figure 3), with the exception of **5LI-IAM-NO₂**, which has relatively low singlet and triplet energies despite the fact that the -NO₂ group is strongly π-withdrawing ($\boldsymbol{R}$ = 0.13). This deviation is explained by the TD-DFT results (*vide infra*). Significantly, the slopes of the correlation lines differ, indicating that the response of the absorption, fluorescence and phosphorescence energies to the effect on the ligand electronic structure caused by the substituents also differs. The substituent influence is greater for the fluorescence energies than for the absorption energies and greater still for the T_{0-0} energies. Consequently, as the π-withdrawing ability of the substituent increases, the singlet and triplet state energies also increase, while the singlet-triplet energy gaps decrease (Figure S18)

To determine how altering the ligand energy levels of the IAM-X chromophores through substitution affects Tb(III) sensitization, the emission spectra of the Tb(III) complexes and the luminescence quantum yields (Φ) were measured. The spectra show the characteristic bands corresponding to transitions from the $^5D_4$ emitting state to the ^7F_J ground state manifold (Figure 2). The luminescence

7

quantum yield values for overall energy transfer for the Tb(III) complexes were measured relative to quinine sulfate (Φ = 0.546).[41] The Φ values range from 0.40 for **Tb-Amide** to 0 for **Tb-OCH$_3$ and Tb-NO$_2$**. From these data it can be seen that generally, the Φ values increase with T_{0-0} (Figure 4), which can be attributed in part to the increase in the $T_{0-0} - {}^5D_4$ energy gap, which decreases non-radiative deactivation caused by repopulation of the triplet *via* back-transfer from the ${}^5D_4$ state (i.e. increased Φ_{ET}).[42] Additionally, for this ligand system, increased T_{0-0} energies are associated with decreased singlet-triplet energy gaps. Moving to more π-withdrawing substituents therefore also influences η_{ISC}. The observed $T_{0-0} - \Phi$ relationship for the **5LI-IAM-X** series is consistent with previous reports relating antenna ligand triplet energies and the quantum yield values of the resulting Tb(III) complexes, which suggest that the antenna triplet levels should be ~1,500 – 1,700 cm^{-1} higher in energy than the Ln(III) emitting state to achieve efficient sensitization.[31,43] For the Tb-5LI-IAM-X complexes, Φ values decrease gradually as the $T_{0-0} - {}^5D_4$ energy gap is lowered from ~ 3,500 cm^{-1} (**Tb-Amide**) to ~ 1,600 cm^{-1} (**Tb-CH$_3$**), and then plummet when the energy gap shrinks to ~ 600 cm^{-1} (**Tb-F**). Latva and coworkers observed a similarly sharp drop-off in quantum yield values as the antenna triplet energies went below ~22000 cm^{-1}.[31] Although looking at energy transfer efficiency only in terms of the antenna triplet levels is an oversimplification of the energy transfer process, the $T_{0-0} - {}^5D_4$ relationship is nonetheless a useful trend to guide ligand design, especially when looking at a single class of antenna ligands.

As previously mentioned, both **Tb-NO$_2$** and **Tb-OCH$_3$** show no metal-based emission. The triplet energy of **5LI-IAM-OCH$_3$** is below the ${}^5D_4$ emitting state and so this ligand is not expected to sensitize Tb(III) emission at room temperature due to competing thermal repopulation of the ligand triplet.[11] As this quenching effect is significantly diminished upon cooling, at 77K Tb(III)-based emission is seen for this complex (Figure S19). The triplet energy of **5LI-IAM-NO$_2$**, however is ~1,000 cm^{-1} above the ${}^5D_4$ emitting state and only ~200 cm^{-1} below the **5LI-IAM-F** triplet state, so it is, at first glance, surprising

that not even weak Tb(III) emission for **Tb-NO₂** is seen at room temperature. This observation, however, can be rationalized based on TD-DFT results (*vide infra*). The photophysical properties of **Tb-Br** are also unexpected, given that the triplet energies of **5LI-IAM-Br** and **5LI-IAM-Cl** are nearly equivalent. We are currently investigating the source of this behavior, which we believe to be a heavy-atom effect of the Br.

Lifetime Measurements. To determine if bound water molecules were contributing the observed variation in quantum yield values, and to better characterize the sensitization process, the lifetimes of the Tb(III) complexes were measured in both H_2O and D_2O at room temperature and at 77K (Table 1). The lifetime data for all of the complexes were fit to mono-exponential decays, which confirm the presence of single Tb(III) emitting species in solution. In H_2O, at room temperature, the **Tb-H**, **Tb-Amide**, **Tb-Cl**, and **Tb-CH₃** complexes display luminescence lifetimes on the order of 2 ms, which are consistent with lifetimes observed for known Tb-IAM complexes.[24] The lifetime of **Tb-SO₃⁻** is significantly shorter, at 1.23 ms. This shortened lifetime is not due to solvent quenching, since the number of bound water molecules (q) estimated from the lifetime data in H_2O and D_2O for this complex is 0.2.[44] Indeed, for these five complexes, the near-zero q values indicate that the 5LI-IAM scaffold effectively protects the Tb(III) ion from direct coordination of solvent. For **Tb-SO₃⁻**, the relatively short lifetime is likely due to a difference in the Tb(III) coordination environment for this complex, in comparison to the others, as indicated by the change in the relative intensities of the $^5D_4 \rightarrow {}^7F_J$ peaks. For **Tb-SO₃⁻**, in contrast to **Tb-H** for example, the intensities of the $^5D_4 \rightarrow {}^7F_{6,4,3,2,1,0}$ transitions relative to the $^5D_4 \rightarrow {}^7F_5$ transition are markedly decreased (Figure 5). For Tb(III), the $^5D_4 \rightarrow {}^7F_{6,4,2}$ transitions in particular show some sensitivity to the Tb(III) coordination environment.[45]

The lifetimes of **Tb-Cl** and **Tb-Me**, at 1.98 and 2.04 ms, respectively, are slightly shortened compared to that of **Tb-H** (2.52 ms), which is consistent with increased back-transfer occurring in these two complexes. That effect is most pronounced for **Tb-F**, whose ligand triplet energy is only ~1,100 cm⁻¹

9

higher in energy than the $^5D_4$ emitting state, and which displays a significantly shortened lifetime of 0.650 ms in H_2O at room temperature. Interestingly, **Tb-Br** also has a relatively short lifetime (0.943 ms) in H_2O at room temperature, although, as mentioned earlier, the **5LI-IAM-Br** triplet state is nearly equivalent in energy to that of **5LI-IAM-Cl** and **Tb-Cl** shows only minor decreases in quantum yield and lifetime compared to **Tb-H**. While the source of **Tb-Br**'s short lifetimes and low quantum yield at room temperature are not completely understood, they do not appear to be due to the presence bound water, but rather to a thermal deactivation pathway. The effect of thermal back-transfer is reflected in the differences in lifetimes observed for the complexes at room temperature and at 77K.[11] For **Tb-Amide**, **Tb-SO₃⁻**, and **Tb-H**, which have the highest quantum yield values and whose ligands have the highest triplet energies, the lifetimes are invariant, within experimental error, upon cooling the sample from room temperature to 77K. **Tb-Me**, **Tb-Cl**, **Tb-F**, and **Tb-Br** in comparison show significant changes in lifetime upon cooling to 77K, which indicates that thermally-induced quenching is occurring with these complexes.

Theoretical Investigation of Ligand Excited States. With the experimental results in hand, time-dependent density functional theory (TD-DFT) calculations were performed using *Gaussian 03*[46] to gain further insight into the how the substituents affect ligand excited states. More importantly, these calculations can serve as a quick screening method to aid in the design of antenna chromophores. In order to simplify the calculations, only one bidentate IAM unit was used in the input structure and the Ln(III) was replaced with Na^+ (Figure 6). Gutierrez *et al.* have previously shown that such structures are reasonable analogs of multidentate Tb(III) complexes in calculations of this nature.[47] They were, however, only able to reproduce relative positions of ligand triplet states as their calculated values were ~ 2,500 cm^{-1} lower in energy than experimental values.[47] To evaluate the accuracy of the calculations, the lowest-energy calculated triplet states were compared to the measured T_1 values for each complex and the calculated singlet states with the largest oscillator strengths were compared to the absorption maxima (λ_{max}^{ab}) of the complexes. The calculated wavelengths are within a few nm of the experimental

values (Table 2), with the exception of the nitro-substituted species, for which the calculated lowest-energy triplet is 31 nm (1,330 cm^{-1}) lower than the measured triplet. Examining the molecular orbitals for the transitions shows that the singlet-singlet and singlet-triplet transitions of the ligands are π-π* in nature, except for the nitro-substituted ligand (**5LI-IAM-NO$_2$**), which has intra-ligand charge transfer (ILCT) contributions (Figure 7). This supports the finding that the ligand T$_{0-0}$ energies correlate to the π-withdrawing/donating ability of the substituent and also provides an explanation for the aberrant behavior of **5LI-IAM-NO$_2$** and its Tb(III) complex; this ligand deviates from the Hammett correlations seen for the other ligands because the electronic transition is different. The presence of an ILCT state for **5LI-IAM-NO$_2$** implies that such states may lie lower in energy than the ligand triplet, or that the emission lifetime is too short to allow for energy transfer to the $^5D_4$ state. At 77K, the ILCT would be higher in energy and longer-lived than at room temperature, as stabilization due to solvent reorganization is slowed, and Tb(III) emission should be observed.[48] Indeed, at 77K, the emission spectrum of **Tb-NO$_2$** (Figure S20) shows metal-based emission. It should be noted that emission of **Tb-NO$_2$** at 77K can, in part, also possibly be attributed to eliminating thermal back transfer, which likely contributes to quenching at room temperature.

Conclusions

Para-substitution of the IAM ligand produces significant changes in the ligand excited state energies and consequent Tb(III) emission. Quantum yield and lifetime measurements of the Tb(III) complexes and low temperature emission studies of the Gd(III) complexes, together with a theoretical study of the ligand series, have provided a clear view of how the substituents ultimately impact Ln(III) emission and help explain the remarkable brightness of Tb-IAM complexes. Overall, the 5LI-IAM-X series provides a quantitative measure of substituent effects on ligand energy levels and on the emission intensity of the corresponding Tb(III) complexes. Time-dependent density functional theory calculations of the Na$^+$

11

analogs of simplified, bidentate ligands reproduce the experimental values with remarkable accuracy. Ultimately, these complementary tools serve as a guide to inform the design of new ligands to produce more highly luminescent lanthanide complexes.

Experimental Section

General

All chemicals were obtained from commercial suppliers and used without further purification unless otherwise noted. Flash silica gel chromatography was performed using Merck 40-70 mesh silica gel. ^{1}H and ^{13}C NMR spectra (recorded at ambient temperature on Bruker FT-NMR spectrometers), elemental analyses, and mass spectra were obtained at the corresponding analytical facility in the College of Chemistry, University of California, Berkeley.

i. 5-Chloro-2-methoxy-1,3-dimethylbenzene (2a): Representative Procedure. 4-Chloro-2,6-dimethylphenol (107 g, 0.683 mol) and K_2CO_3 (220 g, 1.59 mol) were suspended in 2.5 L of acetone. Dimethyl sulfate was added and the solution was heated to reflux overnight. The resulting yellow solution was cooled to room temperature and additional dimethyl sulfate (50 mL, 0.52 mmol) and K_2CO_3 (50 g, 0.36 mmol) were added and the reaction mixture was heated to reflux for 4 h. After cooling, the reaction mixture was filtered and the filtrate was evaporated to dryness. The product was carried to the next step without further purification. Yield: 152 g (97%). ^{1}H NMR (400 MHz, d_6-Acetone): δ 2.88 (s, 3H, OCH$_3$), 3.95 (s, 6H, CH$_3$), 7.01 (s, 2H, ArH) ppm. ^{13}C NMR (100 MHz, d_6-Acetone): δ 15.2, 58.5, 59.1, 127.8, 132.8, 155.8 ppm.

5-Bromo-2-methoxy-1,3-dimethylbenzene (2b). ^{1}H NMR (400 MHz, d_6-Acetone): δ 2.28 (s, 6H, CH$_3$), 3.95 (s, 3H, OCH$_3$), 7.16 (s, 2H, ArH) ppm. ^{13}C NMR (100 MHz, d_6-Acetone): δ 16.0, 59.6, 116.4, 131.5, 133.1, 156.2 ppm.

ii. 5-Chloro-2-methoxybenzene-1,3-dicarboxylic acid (6a): Representative Procedure. To a solution of KOH (9.25 g, 165 mmol) in 3.5 L of water was added 63.4 g (373 mmol) of **2a**. The solution was heated to reflux and KMnO$_4$ (300 g, 1.90 mol) was added in 20 g portions over 7 days. The solution was then filtered and the volume of the filtrate was reduced to 1 L under vacuum. The filtrate was acidified to pH 1 with conc. HCl and cooled to 4 ^{o}C. The resulting white precipitate was collected by filtration and dried. Yield: 42.8 g (50%). ^{1}H NMR (400 MHz, d_6-DMSO): δ 3.77 (s, 3H, OCH$_3$), 7.79 (s, 2H, ArH), 13.45 (s, 2H, COOH) ppm. ^{13}C NMR (100 MHz, d_6-DMSO): δ 63.7, 127.9, 130.2, 133.1, 156.8, 166.2 ppm.

5-Bromo-2-methoxybenzene-1,3-dicarboxylic acid (6b). ^{1}H NMR (400 MHz, d_6-DMSO): δ 3.77 (s, 3H, OCH$_3$), 7.90 (s, 2H, ArH), 13.43 (s, br, 2H, COOH) ppm. ^{13}C NMR (100 MHz, d_6-DMSO): δ 63.6, 115.5, 130.5, 135.9, 157.3, 166.1 ppm. Anal. Calcd. (Found) for C$_9$H$_7$BrO$_5$•H$_2$O: C, 36.88 (36.76); H, 3.10 (3.04) ppm.

iii. (2-Hydroxy-5-methoxy-1,3-phenylene)dimethanol (4d): Representative Procedure. To a solution of NaOH (80 g, 2.0 mol) and 4-methoxyphenol (124 g, 1.0 mol) in water (1 L) was added paraformaldehyde (90 g) slowly, while stirring, so that the solution temperature did not exceed 40 °C. The reaction mixture was stirred for 24 h at 30 °C and was then saturated with sodium sulfate. After standing at 0 °C overnight, the product precipitated out of solution and was collected by filtration, washed with cold water and air dried. Yield: 144 g (78%). ^{1}H NMR (500 MHz, d_6-DMSO): δ 3.66 (s, 3H, CH$_3$), 4.50 (s, 4H, CH$_2$), 6.729 (s, 2H, ArH) ppm. ^{13}C NMR (125 MHz, d_6-DMSO): δ 55.2, 59.1, 110.8, 128.4, 129.8, 144.8, 152.4 ppm.

(5-Fluoro-2-hydroxy-1,3-phenylene)dimethanol (4c). ^{1}H NMR (400 MHz, CDCl$_3$): δ 4.51 (d, 4H, J = 5 Hz, C$\underline{H}_2$OH), 5.29 (t, 2H, J = 5 Hz, CH$_2$O$\underline{H}$), 6.92 (d, 2H, J = 9 Hz, ArH), 8.40 (s, 1H, ArOH) ppm. ^{13}C NMR (100 MHz, CDCl$_3$) δ: 59.0, 111.5, 111.7, 131.3, 131.4, 147.1 ppm. Anal. Calcd. (Found) for C$_8$H$_9$FO$_3$: C, 55.81 (55.95); H, 5.27 (5.42).

iv. (2-(Benzyloxy)-5-fluoro-1,3-phenylene)dimethanol (5c): Representative Procedure. To a solution of 9.0 g (52 mmol) of **4c** in 150 mL of DMF was added 9.5 g (69 mmol) of anhydrous K$_2$CO$_3$ and 5.5 mL (65 mmol) of benzyl chloride while stirring. The reaction mixture was stirred overnight at 75 $^{\circ}$C under N$_2$. The resulting yellow slurry was filtered over celite, the filtrate was collected and its volume was reduced. The resulting yellow residue was applied to a silica column and eluted with ethyl acetate. The product, a yellow solid, was recrystallized (ethyl acetate and hexanes). Yield: 9.9 g (72%). ^{1}H NMR (400 MHz, d_6-DMSO): δ 4.54 (d, 4H, J = 7 Hz, C$\underline{H}_2$OH), 4.81 (s, 2H, CH$_2$Ar), 5.27 (t, 2H, J = 6 Hz, CH$_2$O$\underline{H}$), 7.09 (d, 2H, J = 9 Hz, ArH), 7.38 (m, 5H, ArH) ppm. ^{13}C NMR (100 MHz, d_6-DMSO): δ 58.0, 75.8, 112.9, 113.1, 128.5, 128.5, 128.9, 137.8, 138.2, 138.3, 149.1 ppm. MS (FAB+): *m/z* 262.1 [MH$^+$].

(2-(Benzyloxy)-5-methoxy-1,3-phenylene)dimethanol (5d). ^{1}H NMR (300MHz, CDCl$_3$): δ 2.01 (t, 2H, J = 7 Hz, CH$_2$O$\underline{H}$), 3.80 (s, 3H, OCH$_3$), 4.68 (d, 4H, J = 10 Hz, C$\underline{H}_2$OH), 4.90 (s, 2H, CH$_2$), 6.98 (s, 2H, ArH), 7.35 – 7.45 (m, 5H, ArH) ppm. ^{13}C NMR (125 MHz, d_6-DMSO): δ 55.2, 58.1, 75.6, 111.8, 128.0, 128.5, 136.3, 137.7, 146.6, 155.6 ppm.

v. (2-Methoxy-5-methyl-1,3-phenylene)dimethanol (5e). To a solution of NaOH (49.4 g, 1.23 mmol) in 450 mL of water was added **4e** (136 g, 0.81 mmol). Dimethyl sulfate (79.0 ml, 838 mmol) was added to the resulting brown solution, and the reaction mixture was stirred for ~ 30 min. The solution was then filtered to remove a brown precipitate, the filtrate was returned to the reaction vessel and additional dimethyl sulfate (40.0 ml, 420 mmol) was added in 4 mL aliquots every 5 min. Once the addition was complete, the product, a white precipitate, was collected by filtration and dried. Yield: 104 g (87%). [1]H

NMR (400 MHz, d_6-Acetone): δ 3.70 (s, 3H, CH$_3$), 4.18 (s, 3H, OCH$_3$), 4.62 (s, 4H, C$\underline{H}_2$OH), 7.16 (s, 2H, ArH) ppm. ^{13}C NMR (100 MHz, d_6-Acetone): δ 20.2, 58.8, 61.7, 128.0, 132.8, 134.5, 153.1 ppm.

vi. 2-(Benzyloxy)-5-fluorobenzene-1,3-dicarboxylic acid (6c): Representative Procedure. To a solution of **5c** (4.7 g, 17.9 mmol) in 50 mL of acetone was added 20 mL of Jones Reagent[35] drop-wise over 1 h. The resulting blue-green solution was stirred at room temperature for an additional 5 h, during which time an insoluble dark blue mixture formed. The acetone was removed under reduced pressure and the resulting reside was dissolved in 150 mL of water and extracted with ethyl acetate (3 × 200 mL). The organic layers were combined and dried over MgSO$_4$. After removal of the solvents and recrystallization (MeOH), the product was obtained as an off-white powder. Yield: 3.22 g (63%). ^{1}H NMR (400 MHz, d_6-DMSO): δ 5.01 (s, 2H, CH$_2$Ar), 7.30 (m, 5H, ArH), 7.68 (d, 2H, J = 8 Hz, ArH), 13.55 (s, *br*, 1H, COO$\underline{H}$) ppm. ^{13}C NMR (100 MHz, d_6-DMSO): δ 77.6, 120.1, 120.3, 128.4, 128.7, 130.7, 130.7, 137.4, 152.5, 156.3, 166.4 ppm. MS (FAB+): m/z 291.2 [MH$^+$]. Anal. Calcd. (Found) for C$_{15}$H$_{11}$FO$_5$: C, 62.07 (62.30); H, 3.82 (3.82).

5-Bromo-2-methoxybenzene-1,3-dicarboxylic acid (6d). ^{1}H NMR (500 MHz, CDCl$_3$): δ 3.90 (s, 3H, CH$_3$), 5.15 (s, 2H, ArCH$_2$), 7.42 (m, 3H, ArH), 7.48 (m, 2H, ArH), 7.84 (s, 2H, ArH) ppm. ^{13}C NMR (125 MHz, CDCl$_3$): δ 55.9, 77.0, 118.2, 127.9, 128.2, 128.2, 129.3, 137.3, 149.3, 154.6, 166.9 ppm.

vii. 2-Methoxy-5-methylbenzene-1,3-dicarboxylic acid (6e). A solution of **5e** (55 g, 0.30 mmol) and KOH (5.0 g, 89 mmol) in 1.4 L of water was cooled to 0 °C in an ice bath. KMnO$_4$ (131 g, 0.82 mmol) was added in ~ 10 g portions over several hours. Once the addition was complete, the solution was warmed to room temperature and 1 mL of formaldehyde was added. The solution was then filtered over celite and the filtrate was collected. The volume of the filtrate was reduced under vacuum to ~150 mL and the solution was acidified to pH 1 with conc. HCl. The resulting white precipitate was collected by filtration and dried. Yield: 52 g (67%). ^{1}H NMR (400 MHz, CD$_3$OD): δ 2.41 (s, 3H, CH$_3$), 3.91 (s,

3H, OCH$_3$), 7.80 (s, 2H, ArH) ppm. ^{13}C NMR (100 MHz, CD$_3$OD): δ 20.6, 64.0, 128.2, 134.9, 136.3, 158.5, 169.2 ppm. Anal. Calcd. (Found) for C$_{10}$H$_{10}$O$_5$: C, 57.14 (57.40); H, 4.80 (4.84).

viii. 2-Methoxy-5-nitrobenzene-1,3-dicarboxylic acid (6g). A flask containing **6f** (15.0 g, 76.5 mmol) was cooled to 0 °C. A 1:2 mixture of fuming HNO$_2$:H$_2$SO$_4$ (30 mL total) was added drop-wise over 12 minutes while stirring. The resulting viscous mixture was warmed to room temperature and stirred for 5 h, then poured over crushed ice, causing the product to precipitate out of solution. The solution was filtered and the product washed with cold water. Yield: 13.4 g (73%). ^{1}H NMR (400 MHz, d_6-Acetone): δ 4.00 (s, 2H, OCH$_3$), 8.66 (s, 2H, ArH) ppm. ^{13}C NMR (100 MHz, d_6-Acetone): δ 63.5, 128.0, 129.2, 142.4, 163.9, 164.7 ppm.

ix. (2-Methoxy-5-methyl-1,3-phenylene)bis((2-thioxothiazolidin-3-yl)methanone) (7e): Representative Procedure. To a solution of **6e** (40 g, 0.19 mol) in 250 mL of dry dioxane was added 48 mL (0.66 mol) of thionyl chloride and 2 drops of DMF. The mixture was heated to reflux and stirred overnight under N$_2$. The volatiles were removed under vacuum by co-evaporation with 50 mL of dioxane. The crude acyl chloride was dissolved in 200 mL of CH$_2$Cl$_2$ and a solution of 2-mercaptiothiazoline (50 g, 0.42 mol) and NEt$_3$ (55 mL) in 100 mL of CH$_2$Cl$_2$ was added drop-wise at -78 °C. The reaction mixture was warmed to room temperature and stirred overnight. The resulting yellow reaction mixture was washed with brine (100 mL), 1 M HCL (100 mL), and 1 M NaOH (2 × 100 mL) successively. The solution was then dried over MgSO$_4$ and evaporated to dryness, yielding the product as a bright yellow solid. Yield: 62.0 g (79%). ^{1}H NMR (400 MHz, CDCl$_3$): δ 2.31 (s, 3H, CH$_3$), 3.40 (t, 4H, J = 7 Hz, CH$_2$), 3.84 (s, 3H, OCH$_3$), 4.56 (t, 4H, J = 7 Hz, CH$_2$), 7.22 (s, 2H, ArH) ppm. ^{13}C NMR (100 MHz, CDCl$_3$): δ 20.6, 29.3, 55.8, 63.2, 128.2, 132.5, 133.5, 152.7, 167.4, 200.7 ppm. MS (FAB+): m/z 413 [MH$^+$].

(5-Chloro-2-methoxy-1,3-phenylene)bis((2-thioxothiazolidin-3-yl)methanone) (7a). ^{1}H NMR (300 MHz, CDCl$_3$): δ 3.43 (t, 4H, J = 7 Hz, CH$_2$), 3.87 (s, 3H, OCH$_3$), 4.59 (t, 4H, J = 7 Hz, CH$_2$), 7.35 (s, 2H, ArH) ppm. MS (FAB+): m/z 433 [MH$^+$].

(5-Bromo-2-methoxy-1,3-phenylene)bis((2-thioxothiazolidin-3-yl)methanone) (7b). ^{1}H NMR (400 MHz, CDCl$_3$): δ 1.59 (s, 3H, OCH$_3$), 3.42 (t, 4H, J = 7 Hz, CH$_2$), 3.84 (s, 3H, OCH$_3$), 4.58 (t, 4H, J = 7 Hz, CH$_2$), 7.49 (s, 2H, ArH) ppm. ^{13}C NMR (100 MHz, CDCl$_3$): δ 29.8, 56.4, 62.3, 114.1, 130.4, 133.7, 153.9, 165.7, 202.8 ppm. Anal. Calcd. (Found) for C$_{15}$H$_{13}$BrN$_2$O$_3$S$_4 \cdot$H$_2$O: C, 37.74 (37.66); H, 2.74 (2.97); N, 5.87 (5.64); S, 26.86 (26.47).

(2-Methoxy-5-nitro-1,3-phenylene)bis((2-thioxothiazolidin-3-yl)methanone) (7g). ^{1}H NMR (400 MHz, CDCl$_3$): δ 3.47 (t, 2H, J = 7 Hz, CH$_2$), 3.95 (s, 3H, OCH$_3$), 4.63 (t, 2H, J = 7 Hz, CH$_2$), 8.19 (s, 2H, ArH) ppm. MS (FAB+): m/z 444 [MH$^+$]. Anal. Calcd. (Found) for C$_{15}$H$_{13}$N$_3$O$_5$S$_4$: C, 40.62 (40.50); H, 2.95 (3.12); N, 9.47 (9.20); S, 28.92 (29.10).

x. (2-(Benzyloxy)-5-fluoro-1,3-phenylene)bis((2-thioxothiazolidin-3-yl)methanone) (7c): Representative Procedure. To a suspension of **6c** (5.0 g, 17 mmol) in 100 mL of dry benzene was added 4.0 mL (46 mmol) of oxalyl chloride, along with 2 drops of DMF. The off-white slurry was stirred overnight at 50 ^{o}C under N$_2$, during which the reaction mixture became transparent. The benzene was removed under reduced pressure and the resulting brown residue was dried further under vacuum for 5 hours to remove any remaining oxalyl chloride. The crude acyl chloride was dissolved in 100 mL of dry THF and cooled in an ice bath. A solution of 30 mL of NEt$_3$, 5.12 g (43 mmol) of 2-mercaptothiazoline, and 50 mL of dry THF was added drop-wise while stirring. The reaction mixture was stirred overnight at room temperature. The resultant yellow slurry was filtered over celite. The yellow filtrate was collected and its volume was reduced. The resulting oil was dissolved in CH$_2$Cl$_2$ and washed successively with 1 M HCl (200 ml) and 1 M KOH (200 mL). The organic layer was dried over MgSO$_4$, and further purified on a silica column (CH$_2$Cl$_2$). Yield: 4.66 g (55%). ^{1}H NMR (400 MHz, CDCl$_3$): δ 3.03 (t, 4H, J = 7 Hz, CH$_2$), 4.41 (t, 4H, J = 7 Hz, CH$_2$), 4.99 (s, 2H, J = 6 Hz, CH$_2$Ar), 7.18

17

(s, 1H, ArH), 7.20 (s, 1H, ArH), 7.38 (m, 5H, ArH) ppm. ^{13}C NMR (100 MHz, CDCl$_3$): δ 28.9, 55.6, 118.6, 118.9, 127.5, 128.4, 128.7, 130.5, 136.7, 166.0, 200.6 ppm. MS (FAB+): *m/z* 493.2 [MH$^+$].

(2-(Benzyloxy)-5-methoxy-1,3-phenylene)bis((2-thioxothiazolidin-3-yl)methanone) (7d). ^{1}H NMR (500 MHz, CDCl$_3$): δ 2.99 (t, 4H, *J* = 7 Hz, CH$_2$), 3.74 (s, 3H, OCH$_3$), 4.32 (t, 4H, *J* = 7 Hz, CH$_2$), 4.90 (s, 2H, ArCH$_2$), 6.97 (s, 2H, ArH), 7.2 – 7.4 (m, 7H, ArH) ppm. ^{13}C NMR (125 MHz, CDCl$_3$): δ 28.7, 55.5, 55.7, 77.3, 116.8, 127.2, 128.0, 128.2, 128.9, 136.4, 146.2, 155.2, 166.4, 200.6 ppm.

xi. 2-(Benzyloxy)-5-fluoro-*N*-methyl-3-(2-thioxothiazolidine-3-carbonyl)benzamide (8c): Representative Procedure. To a solution of **7c** (5.0 g, 10.2 mmol) in 5 mL of CH$_2$Cl$_2$ was added a solution of methylamine (0.4 g of a 40% aq. soln.) in 98:2 CH$_2$Cl$_2$:MeOH (200 mL total) via cannula over 48 h. The solvents were removed under reduced pressure and the reaction mixture was dissolved in 100 mL of CH$_2$Cl$_2$ and washed with 150 mL of 1M KOH. The reaction mixture was evaporated to dryness and applied to a silica column. Unreacted starting material was eluted with 100% CH$_2$Cl$_2$, and the product, a thick yellow oil, was eluted with 10% EtOAc in CH$_2$Cl$_2$. Yield: 2.20 g (87%). ^{1}H NMR (400 MHz, CDCl$_3$): δ 2.84 (d, 3H, *J* = 5 Hz, NHCH$_3$), 3.13 (t, 2H, *J* = 7 Hz, CH$_2$), 4.49 (t, 2H, *J* = 7 Hz, CH$_2$), 4.92 (s, 2H, CH$_2$Ar), 7.13 (dd, 1H, *J* = 7, 3 Hz, ArH), 7.30 (m, 5H, ArH), 7.81 (dd, 1H, *J* = 7, 3 Hz, ArH) ppm. ^{13}C NMR (100 MHz, CDCl$_3$): δ 26.6, 28.7, 118.9, 119.2, 120.4, 120.7, 128.0, 128.9, 129.0, 129.5, 129.6, 135.6, 150.0, 157.6, 160.1, 164.1, 166.0, 201.4 ppm. MS (FAB+): *m/z* 405 [MH$^+$].

5-Chloro-2-methoxy-*N*-methyl-3-(2-thioxothiazolidine-3-carbonyl)benzamide (8a). ^{1}H NMR (500 MHz, CDCl$_3$): δ 2.11 (s, 3H, ArCH$_3$), 2.77 (d, 3H, *J* = 5 Hz, NHCH$_3$), 3.24 (t, 2H, *J* = 7 Hz, CH$_2$), 3.62 (s, 3H, OCH$_3$), 4.42 (t, 2H, *J* = 7 Hz, CH$_2$), 7.03 (dd, 1H, *J* = 2, 1 Hz, ArH), 7.35 (q, 1H, *J* = 5 Hz, NHCH$_3$), 7.65 (dd, *J* = 2, 1 Hz, ArH) ppm. ^{13}C NMR (125 MHz, CDCl$_3$): δ 20.4, 26.6, 29.1, 55.7, 63.0, 126.6, 128.8, 132.1, 133.9, 134.1, 153.2, 165.4, 167.3, 201.4 ppm.

5-Bromo-2-methoxy-*N*-methyl-3-(2-thioxothiazolidine-3-carbonyl)benzamide (8b). ^{1}H NMR (400 MHz, CDCl$_3$): δ 2.98 (d, *J* = 5 Hz, 3H, NHCH$_3$), 3.31 (t, 2H, *J* = 7 Hz, CH$_2$), 3.81 (s, 3H, OCH$_3$), 4.63

(t, 2H, J = 7 Hz, CH$_2$), 7.34 (s, 1H, ArH), 7.46 (s, 1H, ArH), 8.19 (s, 1H, N$\underline{H}$CH$_3$) ppm. ^{13}C NMR (100 MHz, CDCl$_3$): δ 26.9, 29.1, 55.5, 63.3, 117.2, 128.9, 131.1, 134.1, 136.6, 154.4, 164.1, 165.8 ppm. MS (FAB+) m/z 391 [MH$^+$].

2-(Benzyloxy)-5-methoxy-*N*-methyl-3-(2-thioxothiazolidine-3-carbonyl)benzamide (8d). ^{1}H NMR (500 MHz, CDCl$_3$): δ 2.82 (dd, 3H, J = 5, 3 Hz, CH$_3$), 3.08 (t, 2H, J = 7 Hz, CH$_2$), 3.80 (s, 3H, OCH$_3$), 4.45 (t, 2H, J = 7 Hz, CH$_2$), 4.87 (s, 2H, ArCH$_2$), 6.96 (s, 2H, ArH), 7.30 – 7.45 (m, 5H, ArH), 7.44 (d, 1H, J = 5 Hz, N$\underline{H}$CH$_3$), 7.63 (s, 2H, ArH) ppm. ^{13}C NMR (125 MHz, CDCl$_3$): δ 26.3, 28.5, 55.5, 55.8, 78.2, 117.5, 118.3, 127.7, 128.2, 128.6, 130.6, 135.7, 147.4, 155.9, 164.9, 166.7, 201.1 ppm. MS (FAB+): m/z 417 [MH$^+$].

2-Methoxy-*N*,5-dimethyl-3-(2-thioxothiazolidine-3-carbonyl)benzamide (8e). ^{1}H NMR (500 MHz, CDCl$_3$): δ 2.11 (s, 3H, ArCH$_3$), 2.76 (d, 3H, J = 5 Hz, NHCH$_3$), 3.23 (t, 2H, J = 7 Hz, CH$_2$), 3.62 (s, 3H, OCH$_3$), 4.40 (t, 2H, J = 7 Hz, CH$_2$), 7.03 (dd, 1H, J = 2, 1 Hz, ArH), 7.39 (q, 1H, J = 5 Hz, N$\underline{H}$CH$_3$), 7.65 (dd, 1H, J = 2, 1 Hz, ArH) ppm. ^{13}C NMR (125 MHz, CDCl$_3$): δ 20.4, 26.6, 29.1, 55.7, 63.0, 126.6, 128.8, 132.1, 133.9, 134.1, 153.2, 165.4, 167.3, 201.4 ppm. MS (FAB+) m/z 325 [MH$^+$].

2-Methoxy-*N*-methyl-3-(2-thioxothiazolidine-3-carbonyl)benzamide (8f). ^{1}H NMR (400 MHz, CDCl$_3$): δ 2.76 (d, 3H, J = 5 Hz, NHC$\underline{H}_3$), 3.38 (t, 2H, J = 8 Hz, CH$_2$), 3.80 (s, 3H, OCH$_3$), 4.58 (t, 2H, J = 8 Hz, CH$_2$), 7.16 (t, 1H, J = 8 Hz, ArH), 7.34 (dd, 1H, J = 8, 2 Hz, ArH), 7.39 (m, *br,* 1H, N$\underline{H}$CH$_3$), 8.04 (dd, 1H, J = 8, 2 Hz, ArH) ppm. MS (FAB+): m/z 311 [MH$^+$].

2-Methoxy-*N*-methyl-5-nitro-3-(2-thioxothiazolidine-3-carbonyl)benzamide (8g). ^{1}H NMR (500 MHz, CDCl$_3$): δ 3.01 (d, 3H, J = 5 Hz, NHC$\underline{H}_3$), 3.49 (t, 2H, J = 7 Hz, CH$_2$), 3.96 (s, 3H, OCH$_3$), 4.68 (t, 2H, J = 7 Hz, CH$_2$), 7.26 (s, 1H, NH), 8.18 (d, 1H, J = 3 Hz, ArH), 8.87 (d, 1H, J = 3 Hz, ArH) ppm. ^{13}C NMR (125 MHz, CDCl$_3$): δ 27.0, 29.0, 55.4, 65.1, 126.4, 128.1, 128.9, 129.5, 142.0, 159.6, 163.5, 165.2, 201.8 ppm. MS (FAB+): m/z 356 [MH$^+$]. Anal. Calcd. (Found) for C$_{13}$H$_{13}$N$_3$O$_5$S$_2$: C, 43.93 (44.12); H, 3.69 (3.95); N, 11.82 (11.77); S, 18.05 (18.06).

xii. $N^1,N^{1'}$-(pentane-1,5-diyl)bis(5-bromo-2-methoxy-N^3-methylbenzene-1,3-dicarbamide) **(9b):**

Representative Procedure. To a solution of **8b** (6.5 g, 17 mmol) in 150 mL of CH_2Cl_2, 1,5-diaminopentane (0.75 g, 7.3 mmol) in 100 mL of CH_2Cl_2 was added drop-wise over 12 h. The solution was stirred overnight. The solvents were removed under vacuum and the resulting residue was applied to a silica gel column. The product, a white solid, was eluted with 5% MeOH in CH_2Cl_2. Yield: 3.3 g (74%). ^{1}H NMR (400 MHz, CDCl$_3$.): δ 1.47 (m, 2H, CH$_2$), 1.66 (q, 4H, J = 7 Hz, CH$_2$), 2.99 (d, 6H, J = 5 Hz, NHC$\underline{H}_3$) 3.45 (td, 4H, J = 7, 6 Hz, CH$_2$), 3.81 (s, 6H, OCH$_3$), 7.32 (q, 2H, J = 5 Hz, N$\underline{H}$CH$_3$), 7.43 (t, 2H, J = 6 Hz, NH) 8.03 (s, 2H, ArH), 8.08 (s, 2H, ArH) ppm. ^{13}C NMR (100 MHz, CDCl$_3$): δ 24.2, 26.9, 29.1, 39.7, 63.5, 118.2, 129.8, 136.6, 154.6, 163.8, 164.4 ppm. MS (FAB+): m/z 643 [MH$^+$]. Anal. Calcd. (Found) for $C_{25}H_{30}Br_2N_4O_6$: C, 46.75 (46.66); H, 4.71 (4.65); N, 8.72 (8.91).

$N^1,N^{1'}$-(pentane-1,5-diyl)bis(5-chloro-2-methoxy-N^3-methylbenzene-1,3-dicarbamide) **(9a).** ^{1}H NMR (400 MHz, CDCl$_3$): δ 1.50 (m, 2H, CH$_2$), 1.67 (p, 4H, J = 7 Hz, CH$_2$), 2.90 (d, 6H, J = 4 Hz, NHC$\underline{H}_3$), 3.86 (s, 6H, OCH$_3$), 7.72 (d, 1H, J = 3 Hz, ArH), 7.76 (d, 1H, J = 3 Hz, ArH), 7.81 (m, 4H, N$\underline{H}$) ppm. MS (FAB+): m/z 553 [MH$^+$]

$N^1,N^{1'}$-(pentane-1,5-diyl)bis(2-(benzyloxy)-5-fluoro-N^3-methylbenzene-1,3-dicarbamide) **(9c).** ^{1}H NMR (400 MHz, d_6-DMSO): δ 1.24 (m, 2H, CH$_2$), 1.38 (m, 4H, CH$_2$), 2.74 (d, 6H, J = 4 Hz, NHC$\underline{H}_3$), 3.14 (m, 4H, CH$_2$), 4.95 (s, 4H, CH$_2$), 7.35 (m, 14H, ArH), 8.77 (m, 4H, NH) ppm. ^{13}C NMR (100 MHz, d_6-DMSO): δ 24.0, 26.1, 28.6, 77.3, 116.8, 117.0, 128.2, 128.3, 133.3, 133.4, 136.4, 149.1, 164.5, 165.0 ppm. MS (FAB+): m/z 637 [MH$^+$].

$N^1,N^{1'}$-(pentane-1,5-diyl)bis(2-(benzyloxy)-5-methoxy-N^3-methylbenzene-1,3-dicarbamide) **(9d).** ^{1}H NMR (500 MHz, CDCl$_3$,): δ 1.26 (q, 2H, J = 4 Hz, CH$_2$), 2.08 (q, 2H, J = 4 Hz, CH$_2$), 2.78 (d, 3H, J = 3 Hz, CH$_3$), 3.32 (q, 2H, J = 4 Hz, CH$_2$), 3.79 (s, 6H, CH$_3$), 4.84 (s, 4H, CH$_2$), 7.30 (d, 4H, J = 4 Hz, ArH), 7.35 – 7.38 (m, 8H, ArH), 7.47 (t, 2H, J = 7 Hz, NH), 7.53 (q, 4H, J = 2, ArH) ppm. ^{13}C NMR (125 MHz, CDCl$_3$): δ 24.2, 26.5, 28.9, 39.7, 55.8, 79.2, 118.66, 118.9, 128.5, 128.9, 129.1, 129.3,

129.4, 135.1, 147.6, 156.1, 164.9, 165.5 ppm.   MS (FAB+): m/z 697 [MH$^+$].

$N^1,N^{1'}$-(pentane-1,5-diyl)bis(2-methoxy-N^3,5-dimethylbenzene-1,3-dicarbamide) (9e). ^{1}H NMR (300 MHz, CDCl$_3$,): δ 1.50 (q, 2H, J = 5 Hz, CH$_2$), 1.64 (q, 2H, J = 5 Hz, CH$_2$), 2.30, (s, 6H, ArCH$_3$), 3.39 (d, 3H, J = 4 Hz, CH$_3$), 3.32 (q, 2H, J = 5 Hz, CH$_2$), 3.80 (s, 6H, CH$_3$), 7.59 (s, 2H, ArH), 7.61 (s, 2H, ArH), 7.73 (s, 2H, NH), 7.78 (s, 2H, ArH) ppm. ^{13}C NMR (75 MHz, CDCl$_3$): δ 19.7, 24.2, 25.8, 39.2, 62.7, 129.0, 129.3, 132.8, 133.6, 153.7, 165.0 ppm. MS (FAB+): m/z 513 [MH$^+$]. Anal. Calcd. (Found) for C$_{27}$H$_{36}$N$_6$O$_6$: C, 63.26 (63.11); H, 7.08 (7.04); N, 10.93 (10.86).

$N^1,N^{1'}$-(pentane-1,5-diyl)bis(2-methoxy-N^3-methylbenzene-1,3-dicarbamide) (9f). ^{1}H NMR (500 MHz, CDCl$_3$): δ 1.49 (q, 2H, J = 8 Hz, CH$_2$), 1.69 (q, 4H, J = 8 Hz, CH$_2$), 3.02 (d, 6H, J = 5 Hz, CH$_3$), 3.48 (q, 4H, J = 7 Hz, CH$_2$), 3.82 (s, 6H, CH$_3$), 7.25 (t, 2H, J = 8 Hz, ArH), 7.31 (q, 2H, J = 6 Hz, NHCH$_3$), 7.46 (t, 2H, J = 6 Hz, NHCH$_2$), 7.98 (dd, 2H, J = 8, 2 Hz, ArH), 8.02 (dd, 2H, J = 8, 2 Hz, ArH) ppm. ^{13}C NMR (125 MHz, CDCl$_3$): δ 24.5, 26.0, 28.4, 38.9, 62.3, 123.7, 127.5, 127.7, 132.5, 132.5, 155.0, 164.8, 165.4 ppm. MS (FAB+): m/z 485 [MH$^+$].

$N^1,N^{1'}$-(pentane-1,5-diyl)bis(2-methoxy-N^3-methyl-5-nitrobenzene-1,3-dicarbamide) (9g). ^{1}H NMR (400 MHz, CDCl$_3$): δ 1.52 (m, 2H, CH$_2$), 1.69 (q, 4H, J = 7 Hz, CH$_2$), 2.93 (d, 6H, J = 5 Hz, NHCH$_3$), 4.02 (s, 6H, OCH$_3$), 8.00 (m, 4H, NH), 8.50 (d, 2H, J = 3 Hz, ArH), 8.55 (d, 2H, J = 7 Hz, ArH) ppm. MS (FAB+): m/z 575 [MH$^+$].

$N^1,N^{1'}$-(pentane-1,5-diyl)bis(2-methoxy-N^3,N^5-dimethylbenzene-1,3,5-tricarboxamide) (9h). ^{1}H NMR (500 MHz, CDCl$_3$): δ 1.40 (q, 2H, J = 8 Hz, CH$_2$), 1.56 (q, 4H, J = 8 Hz, CH$_2$), 2.75 (d, 6H, J = 5 Hz, CH$_3$), 2.78 (d, 6H, J = 5 Hz, CH$_3$), 3.26 (q, 2H, J = 7 Hz, CH$_2$), 3.79 (s, 6H, CH$_3$), 7.98 (d, 4H, J = 3 Hz, ArH), 8.02 (d, 4H, J = 3 Hz, ArH), 8.31 (q, 2H, J = 7 Hz, NHCH$_3$), 8.39 (t, 2H, J = 6 Hz, NHCH$_2$), 8.55 (q, 2H, J = 5 Hz, NHCH$_3$) ppm. ^{13}C NMR (125 MHz, CDCl$_3$): δ 23.9, 25.5, 26.3, 26.4, 28.7, 62.1, 62.2, 129.1, 129.7, 129.7, 130.0, 130.5, 156.7, 165.1, 165.5, 166.0 ppm. MS (FAB+): m/z 599.3 [MH$^+$].

xiii. $N^1,N^{1'}$-(pentane-1,5-diyl)bis(2-hydroxy-N^3,N^5-dimethylbenzene-1,3,5-tricarboxamide) - 5LI-IAM-(C=O)NHCH$_3$ (10h): Representative Procedure. To a solution of **9h** in 30 mL of CH$_2$Cl$_2$

cooled in an acetone/dry ice bath was added 2.0 mL (22.8 mmol) of BBr_3 with a syringe while stirring. The reaction mixture was warmed to room temperature and was stirred for 64 hours. The progress of the reaction was monitored with ^{1}H NMR. Once the reaction was complete, the volatiles were removed under vacuum. The resulting off-white residue was dissolved in 10 mL of MeOH. The MeOH solution was diluted with 40 mL of water and heated until a transparent solution was obtained and the volume had been reduced to ~ 10 mL. Upon cooling the product precipitated out of solution and was collected by filtration and dried. Yield: 70%. ^{1}H NMR (500 MHz, d_6-DMSO): δ 1.37 (q, 2H, J = 7 Hz, CH_2), 1.58 (q, 4H, J = 7.0 Hz, CH_2), 2.76 (d, 6H, J = 5 Hz, CH_3), 2.82 (d, 6H, J = 5 Hz, CH_3), 3.31 (q, 4H, J = 7, CH_2), 8.84 (m, br, 4H + 2H, ArH + N$\underline{H}CH_2$), 8.80 (q, 2H, J = 5 Hz, N$\underline{H}CH_3$), 8.86 (q, 2H, J = 5 Hz, N$\underline{H}CH_3$) ppm. MS (FAB+): m/z 571 [MH$^+$]. Anal. Calcd. (Found) for $C_{27}H_{34}N_6O_8 \bullet 4H_2O$: C, 50.46 (50.38); H, 6.58 (6.28); N, 13.07 (13.09).

$N^1,N^{1'}$-(pentane-1,5-diyl)bis(5-chloro-2-hydroxy-N^3-methylbenzene-1,3-dicarbamide) - 5LI-IAM-Cl (10a). ^{1}H NMR (400 MHz, d_6-DMSO): δ 1.40 (m, 2H, CH_2), 1.60 (m, 4H, CH_2), 2.82 (d, 6H, J = 4 Hz, NHC$\underline{H}_3$), 3.31 (m, 4H, CH_2), 7.00 (m, 4H, ArH), 8.77 (m, 4H, NH), 14.860 (s, 2H, ArOH) ppm. MS (FAB+): m/z 525 [MH$^+$]. Anal. Calcd. (Found) for $C_{23}H_{26}Cl_2N_4O_6$: C, 52.58 (52.30); H, 4.99 (4.88); N, 10.66 (10.47).

$N^1,N^{1'}$-(pentane-1,5-diyl)bis(5-bromo-2-hydroxy-N^3-methylbenzene-1,3-dicarbamide) - 5LI-IAM-Br (10b). ^{1}H NMR (300 MHz, d_6-DMSO): δ 1.40 (m, 2H, CH_2), 1.56 (m, 4H, CH_2), 2.81 (d, 6H, J = 5 Hz, NHC$\underline{H}_3$), 3.30 (m, 4H, CH_2), 7.81 (m, 4H, ArH), 8.70 (m, 4H, NH), 14.66 (s, 2H, ArOH) ppm. MS (FAB+): m/z 613 [MH$^+$]. Anal. Calcd. (Found) for $C_{23}H_{26}Br_2N_4O_6$: C, 44.97 (44.73); H, 4.27 (4.47); N, 9.12 (8.81).

$N^1,N^{1'}$-(pentane-1,5-diyl)bis(2-hydroxy-N^3,5-dimethylbenzene-1,3-dicarbamide) - 5LI-IAM-CH$_3$ (10e). ^{1}H NMR (400 MHz, d_6-DMSO): δ 1.45 (m, 2H, CH_2), 1.61 (m, 4H, CH_2), 2.82 (d, 6H, J = 4 Hz, NHC$\underline{H}_3$), 3.29 (m, 4H, CH_2N), 7.79 (m, 4H, ArH), 8.77 (m, 4H, NH), 14.65 (s, 2H, ArOH) ppm. MS

(FAB+): m/z 485 [MH$^+$]. Anal. Calcd. (Found) for $C_{25}H_{32}N_4O_6 \cdot H_2O$: C, 59.75 (59.81); H, 6.82 (6.82); N, 11.15 (11.08).

$N^1,N^{1'}$-(pentane-1,5-diyl)bis(2-hydroxy-N^3-methylbenzene-1,3-dicarbamide) - 5LI-IAM-H (10f). ^{1}H NMR (500 MHz, d_6-DMSO): δ 1.36 (q, 2H, $J = 8$, CH$_2$), 1.57 (q, 4H, $J = 8$, CH$_2$), 2.81 (d, 6H, $J = 5$, CH$_3$), 3.30 (q, 4H, $J = 7$, CH$_2$), 3.82 (s, 6H, CH$_2$), 6.95 (t, 2H, $J = 8$ Hz, ArH), 7.31 (dd, 4H, $J = 8$, 2 Hz, ArH), 7.46 (m, 4H, NH) ppm. MS (FAB+): m/z 457 [MH$^+$]. Anal. Calcd. (Found) for $C_{23}H_{28}N_4O_6 \cdot H_2O$: C, 58.22 (58.34); H, 6.37 (6.59); N, 11.81 (11.78).

$N^1,N^{1'}$-(pentane-1,5-diyl)bis(2-hydroxy-N^3-methyl-5-nitrobenzene-1,3-dicarbamide) 5LI-IAM-NO$_2$ (10g). ^{1}H NMR (300 MHz, d_6-DMSO): δ 1.40 (m, 2H, CH$_2$), 1.60 (m, 4H, CH$_2$), 2.82 (d, 6H, $J = 4$ Hz, NHC$\underline{H}_3$), 3.34 (m, 4H, CH$_2$N), 8.82 (m, 4H, ArH), 9.30 (m, br, 4H, NH) ppm. MS (FAB+): m/z 547 [MH$^+$]. Anal. Calcd. (Found) for $C_{23}H_{26}N_6O_{10} \cdot H_2O$: C, 49.13 (48.94); H, 5.00 (4.81); N, 14.89 (15.10).

xiv. $N^1,N^{1'}$-(pentane-1,5-diyl)bis(5-fluoro-2-hydroxy-N^3-methylbenzene-1,3-dicarbamide) - 5LI-IAM-F (10c). To a solution of **9c** (2.0 g, 2.97 mmol) in 25 mL of acetic acid was added 25 mL of conc. HCl and the reaction mixture was stirred for 48 h at room temperature. A white precipitate formed, and was collected by filtration and dried. The filtrate was reduced in volume and a second crop of product was collected. Yield: 1.24 g (85%). ^{1}H NMR (400 MHz, d_6-DMSO): δ 1.37 (m, 2H, CH$_2$), 1.56 (m, 4H, CH$_2$), 2.82 (d, 6H, $J = 4$ Hz, NHC$\underline{H}_3$), 3.29 (m, 4H, CH$_2$), 7.79 (m, 4H, ArH), 8.77 (m, br, 4H, NH), 14.65 (s, 2H, ArOH) ppm. ^{13}C NMR (100 MHz, d_6-DMSO): δ 23.6, 26.2, 28.3, 118.4, 118.7, 119.3, 119.4, 152.4, 154.8, 155.8, 165.9, 166.33 ppm. MS (FAB+): m/z 493 [MH$^+$]. Anal. Calcd. (Found) for $C_{23}H_{26}F_2N_4O_6$: C, 56.06 (55.84); H, 5.32 (5.31); N, 11.38 (11.40).

xv. $N^1,N^{1'}$-(pentane-1,5-diyl)bis(2-hydroxy-5-methoxy-N^3-methylbenzene-1,3-dicarbamide) - 5LI-IAM-OCH$_3$ (10d). To a solution of **9d** (0.35 g, 0.5 mmol) in 25 mL of a 1:1 mixture of glacial acetic acid and MeOH was added 0.1 g of Pd/C catalyst (palladium, 10 wt. % on activated carbon). The

mixture was hydrogenated (atmospheric pressure, room temperature) overnight. The catalyst was removed by filtration, and the filtrate was evaporated to dryness to give the product as a beige solid. Yield: 0.22 g (85%). ^{1}H NMR (500 MHz, DMSO-d_6,): δ 1.35 (q, 2H, J = 8 Hz, CH$_2$), 1.57 (q, 4H, J = 7 Hz, CH$_2$), 2.81 (d, 6H, J = 5 Hz, CH$_3$), 3.30 (q, 4H, J = 7 Hz, CH$_2$), 3.74 (s, 6H, OCH$_3$), 7.29 (dd, 4H, J = 6, 3 Hz, ArH), 8.77 (m, 4H, NH) ppm. ^{13}C NMR (500 MHz, CDCl$_3$): δ 23.9, 26.2, 28.5, 55.9, 117.7, 117.9, 118.6, 118.8, 150.7, 153.6, 166.6, 167.3 ppm. MS (FAB+): m/z 517 [MH$^+$].

xvi: 5,5'-(pentane-1,5-diylbis(azanediyl))bis(oxomethylene)bis(4-hydroxy-3-(methylcarbamoyl) benzenesulfonic acid) - 5LI-IAM-SO$_3$H (10i). 9f (474 mg, 1 mmol) was dissolved in 30% fuming sulfuric acid (10 mL) while stirring in a 25 mL round bottom flask. After being stirred for 18 h, the reaction mixture was poured onto crushed ice (20 g) while being cooled in an ice/NaCl bath causing the product to precipitate out of solution. The product was collected by filtration and washed successively with cold MeOH and Et$_2$O. Yield: 510 mg (81%). ^{1}H NMR (500 MHz, d_6-DMSO): δ 1.35 (q, 2H, J = 7 Hz, CH$_2$), 1.57 (q, 4H, J = 7 Hz, CH$_2$), 2.80 (d, 6H, J = 5 Hz, CH$_3$), 3.28 (q, 4H, J = 6 Hz, CH$_2$), 8.25 (d, 4H, J = 10 Hz, ArH), 8.79 (s, 2H, ArH), 8.96 (m, 2H, NH) ppm. ^{13}C NMR (100 MHz, D$_2$O): δ 23.4, 25.9, 27.9, 39.3, 115.5, 118.1, 128.6, 130.3, 133.3, 160.5, 166.4, 167.6 ppm. MS (FAB+): m/z 617 [MH$^+$]. Anal. Calcd. (Found) for C$_{23}$H$_{28}$N$_4$O$_{12}$S$_2$•H$_2$O: C 43.53(43.90); H 4.76(4.81); N 8.83 (8.74); S 10.11 (9.72).

General Procedure for the Synthesis of Gd(III) Complexes

To a solution of 0.05 mmol of ligand in 10 mL of MeOH was added 1.25 mL of a 20 mM solution (0.025 mmol) of GdCl$_3$•6H$_2$O. 40 μL of pyridine or sym.-collidine were added while stirring and the reaction mixture was heated to reflux for 24 h. The solvents were removed under reduced pressure and the resulting off-white residue was re-dissolved in a minimal amount of MeOH. The product was precipitated out of solution with Et$_2$O and the precipitate was filtered and dried.

[Gd(5LI-IAM-H)$_2$]$^-$: MS (ES-): *m/z* 1068.1 [M$^-$]. **[Gd(5LI-IAM-F)$_2$]$^-$:** MS (ES-): *m/z* 1136.2 [M$^-$].

Anal. Calcd. (Found) for $C_{46}H_{40}F_4GdN_8O_{12} \cdot Na^+ \cdot NaCl \cdot 9H_2O$: C, 39.98 (39.80); H, 4.81 (4.52); N,

8.11(8.08). **[Gd(5LI-IAM-OCH$_3$)$_2$]$^-$:** MS (ES-): *m/z* 1186.3 [M$^-$]. **[Gd(5LI-IAM-(C=O)NHCH$_3$)$_2$]$^-$:**

MS (ES-): *m/z* 1294.4 [M$^-$]. **[Gd(5LI-IAM-CH$_3$)$_2$]$^-$:** MS (ES-): *m/z* 1122.3 [M$^-$]. Anal. Calcd.

(Found) for $C_{50}H_{60}GdN_8O_{12} \cdot Na^+ \cdot 2NaCl \cdot 6H_2O \cdot CH_3OH$: C, 43.80 (43.40); H, 5.19 (4.89); N, 8.01 (7.99).

[Gd(5LI-IAM-Cl)$_2$]$^-$: MS (ES-): *m/z* 1204.1 [M$^-$]. Anal. Calcd. (Found) for

$C_{46}H_{48}Cl_4GdN_8O_{12} \cdot Na^+ \cdot NaCl \cdot 8H_2O \cdot CH_3OH$: C, 38.65 (38.90); H, 4.51 (4.29); N, 7.84 (7.56).

[Gd(5LI-IAM-NO$_2$)$_2$]$^-$: MS (ES-): *m/z* 1248.2 [M$^-$]. Anal. Calcd. (Found) for

$C_{46}H_{48}GdN_{12}O_{20} \cdot Na^+ \cdot NaCl \cdot 6H_2O$: C, 38.47 (38.35); H, 4.21 (4.30); N, 11.71 (11.24). **[Gd(5LI-IAM-**

SO$_3$)$_2$]$^{5-}$: Anal. Calcd. (Found) for $C_{46}H_{48}GdN_8O_{24}S_4 \cdot 3C_5H_7N^+ \cdot Na^+ \cdot 9H_2O$: C, 40.52 (40.49); H, 4.68

(4.54); N, 8.52 (8.46). **[Gd(5LI-IAM-Br)$_2$]$^-$:** MS (ES-): *m/z* 1381.9 [M$^-$]. Calcd. (Found) for

$C_{46}H_{48}Br_4GdN_8O_{12} \cdot Na^+ \cdot NaCl \cdot 7H_2O$: C, 34.76 (34.82); H, 3.93 (3.76); N, 7.05 (6.82).

Photophysical Measurements. Absorption spectra were recorded on a Cary 300 UV-Visible

spectrophotometer using a 1 cm quartz cell. Emission spectra were recorded on a FluoroLog - 3

(JobinYvon) fluorimeter using a 1 cm Supracil quartz luminescence cell (room-temperature

measurements). The Tb(III) complexes (10μM) were prepared *in situ* in 0.1M Tris buffered H_2O (pH

7.4) with 0.2% DMSO. Quantum yields were determined by the optically dilute method[49] using the

following equation:

$$Q_x/Q_r = [A_r(\lambda_r)/A_x(\lambda_x)][I(\lambda_r)/I(\lambda_x)][n_x^2/n_r^2][D_x/D_r]$$

where *A* is the absorbance at the excitation wavelength (λ), *I* is the intensity of the excitation light at the

same wavelength, *n* is the refractive index and *D* is the integrated intensity. Quinine sulfate in 1.0 *N*

sulfuric acid was used as the reference (Q_r = 0.546).[41] Low temperature (77K) emission

(phosphorescence) spectra of Gd(III) complexes were recorded on a Cary Eclipse fluorimeter. The Gd(III) complex solutions were prepared from the isolated complexes (in 1: 4 MeOH:EtOH).[50]

DFT Calculations. Computational studies were conducted at the Molecular Graphics and Computation Facility, College of Chemistry, University of California, Berkeley. Density functional theory and time-dependent density functional theory calculations were performed using a B3LYP/6-311++G(d,p) basis set in Gaussian 03. The input structure was derived from the crystal structure of a previously reported IAM-Eu(III) complex (CSD reference code: EMEVUN).[22] Geometry optimizations were performed on the input structures without symmetry constraints.

Acknowledgements

Supporting Information

Full citation for reference 47. Room temperature absorption and emission spectra of the Tb(III) complexes as well as low temperature (77K) emission spectra of the Gd(III) complexes. Also, the low-temperature emission spectra of **Tb-NO$_2$ and Tb-OCH$_3$** This material is available free of charge via the Internet at http://pubs.acs.org.

References

(1)   Lavis, L. D.; Raines, R. T. *ACS Chem. Biol.* **2008**, *3*, 142-155.

26

(2)   Ulrich, G.; Ziessel, R.; Harriman, A. *Angew. Chem. Int. Ed.* **2008**, *47*, 1184-1201.

(3)   Zimmer, M. *Chem. Rev.* **2001**, *102*, 759-781.

(4)   Giepmans, B. N. G.; Adams, S. R.; Ellisman, M. H.; Tsien, R. Y. *Science* **2006**, *312*, 217-224.

(5)   Lo, K. K.-W. In *Photofunctional Transition Metal Complexes*; Springer Berlin/Heidelberg: 2007; Vol. 123, p 205-245.

(6)   Bunzli, J.-C.; Piguet, C. *Chem. Soc. Rev.* **2005**, *34*, 1048-1077.

(7)   Medintz, I. L.; Uyeda, H. T.; Goldman, E. R.; Mattoussi, H. *Nat. Mater.* **2005**, *4*, 435-446.

(8)   Fu, A.; Gu, W.; Larabell, C.; Alivisatos, A. P. *Curr. Opin. Neurobiol.* **2005**, *15*, 568-575.

(9)   Michalet, X.; Pinaud, F. F.; Bentolila, L. A.; Tsay, J. M.; Doose, S.; Li, J. J.; Sundaresan, G.; Wu, A. M.; Gambhir, S. S.; Weiss, S. *Science* **2005**, *307*, 538-544.

(10)   Hemmila, I.; Laitala, V. *J. Fluor.* **2005**, *15*, 529-542.

(11)   Sabbatini, N.; Guardigli, M.; Lehn, J.-M. *Coord. Chem. Rev.* **1993**, *123*, 201-228.

(12)   Mukkala, V.-M.; Kankare, J. J. *Helv. Chim. Acta* **1992**, *75*, 1578-1592.

(13)   Alpha, B.; Lehn, J.-M.; Mathis, G. *Angew. Chem. Int. Ed.* **1987**, *26*, 266-167.

(14)   Alpha, B.; Balzani, V.; Lehn, J.-M.; Perathoner, S.; Sabbatini, N. *Angew. Chem. Int. Ed.* **1987**, *26*, 1266-1267.

(15)   Charbonniere, L. J.; Balsiger, C.; Schenk, K. J.; Bunzli, J.-C. G. *J. Chem. Soc., Dalton Trans.* **1998**, 505-510.

(16)   Bunzli, J.-C. G.; Ihringer, F. *Inorg. Chim. Acta* **1996**, *246*, 195-205.

(17)   Bunzli, J.-C. G.; Froidevaux, P.; Harrowfield, J. M. *Inorg. Chem.* **1993**, *32*, 3306-3311.

(18)   George, M. R.; Golden, C. A.; Grossel, M. C.; Curry, R. J. *Inorg. Chem.* **2006**, *45*, 1739-1744.

(19)   Lamture, J. B.; Zhou, Z. H.; Kumar, A. S.; Wensel, T. G. *Inorg. Chem.* **1995**, *34*, 864-869.

(20)   de Sa, G. F.; Malta, O. M.; Donega, C. D.; Simas, A. M.; Longo, R. L.; Santa-Cruz, P. A.; de Silva, E. F. *Coord. Chem. Rev.* **2000**, *196*, 165-195.

(21)   Deandrade, A. V. M.; Dacosta, N. B.; Simas, A. M.; Desa, G. F. *Chem. Phys. Lett.* **1994**, *227*, 349-353.

(22)   Petoud, S.; Cohen, S. M.; Bunzli, J.-C.; Raymond, K. *J. Am. Chem. Soc.* **2003**, *125*, 13324-13325.

(23)   Petoud, S.; Muller, G.; Moore, E. G.; Xu, J.; Sokolnicki, J.; Riehl, J. P.; Le, U. N.; Cohen, S. M.; Raymond, K. N. *J. Am. Chem. Soc.* **2007**, *129*, 77-83.

(24)   Seitz, M.; Moore, E. G.; Ingram, A. J.; Muller, G.; Raymond, K. N. *J. Am. Chem. Soc.* **2007**, *129*, 15468-15470.

(25)   http://www.lumiphore.com.

(26)   Chen, J.; Selvin, P. R. *J. Photochem. Photobiol.* **2000**, *135*, 27-32.

(27)   Deum, R. V.; Fias, P.; Driesen, K.; Binnemans, K.; Gorller-Walrand, C. *Phys. Chem. Chem. Phys* **2003**, *5*, 2754-2757.

(28)   de Bettencourt-Dias, A. *Inorg. Chem.* **2005**, *44*, 2734-2741.

(29)   de Bettencourt-Dias, A.; Viswanathan, S. *Dalton Trans.* **2006**, *34*, 4093-4103.

(30)   Guillaumont, D.; Bazin, H.; Benech, J.-M.; Boyer, M.; Mathis, G. *Chem. Phys. Chem.* **2007**, *8*, 480-488.

(31)   Latva, M.; Takalo, H.; Mukkala, V.-M.; Matachescu, C.; Rodriguez-Ubis, J. C.; Kankare, J. *J. Lumin.* **1997**, *75*, 149-169.

(32)   Sato, N.; Shinkai, S. *J. Chem. Soc. Perkin Trans. 2* **1993**, *4*, 621-624.

(33)   Shi, M.; Li, F.; Yi, T.; Zhang, D.; Hu, H.; Huang, C. *Inorg. Chem.* **2005**, *44*, 8929-8936.

(34)   Beeby, A.; Bushby, L. M.; Maffeo, D.; Williams, J. A. G. *J. Chem. Soc., Dalton Trans.* **2002**, *1*, 48-54.

(35)   Slama, J.; Rando, R. R. *Carbohydr. Res.* **1981**, *88*, 213-221.

(36)   Raymond, K. N.; Petoud, S.; Cohen, S. M.; Xu, J. USA, 2003; Vol. 6515113 B2.

(37)   Ross, D. L.; Reissner, E. *J. Org. Chem* **1966**, *31*, 2571-2580.

(38)   Alpha, B.; Ballardini, R.; Balzani, V.; Lehn, J.-M.; Perathoner, S.; Sabbatini, N. *Photochem. Photobiol.* **1990**, *52*, 299-309.

(39)   Hansch, C.; Leo, A.; Taft, R. W. *Chem. Rev.* **1991**, *91*, 165-195.

(40)   Liddle, B. J.; Silva, R. M.; Morin, T. J.; Macedo, F. P.; Shukla, R.; Lindeman, S. V.; Gardinier, J. R. *J. Org. Chem* **2007**, *72*, 5637-5646.

(41)   Meech, S. R.; Philips, D. *J. Photochem.* **1983**, *23*, 193-217.

(42)   Sato, S.; Wada, M. *Bull. Chem. Soc. Japan* **1970**, *43*, 1955-1962.

(43)   Leonard, J. P.; Nolan, C. B.; Stomeo, F.; Gunnlaugsson, T. In *Topics in Current Chemistry*; Springer-Verlag Berlin: Berlin, 2007; Vol. 281, p 1-43.

(44)   Beeby, A.; Clarkson, I. M.; Dickins, R. S.; Faulkner, S.; Parker, D.; Royle, L.; Sousa, A. S. d.; Williams, J. A. G.; Woods, M. *J. Chem. Soc. Perkin Trans. 2* **1999**, 493-503.

(45)   Bunzli, J.-C. G. In *Lanthanide Probes in Life, Chemical and Earth Sciences: Theory and Practice*; Bunzli, J.-C. G., Choppin, G. R., Eds.; Elsevier: Amsterdam, 1989.

(46)   Frisch, M. J. *et al. Gaussian 03*; revision C.01 ed.; Gaussian, Inc: Wallingford, CT, 2004.

(47)   Gutierrez, F.; Tedeschi, C.; Maron, L.; Daudey, J. P.; Azema, J.; Tisnes, P.; Picard, C.; Poteau, R. *THEOCHEM* **2005**, *756*, 151-162.

(48)   Lackowicz, J. R. *Principles of Fluorescence Spectroscopy*; 2nd ed.; Kluwer Academic/Plenum Publishers: New York, 1999.

(49)   Crosby, G. A.; Demas, J. N. *J. Phys. Chem.* **1971**, *75*, 991-1024.

(50)   Scott, D. R.; Allison, J. B. *J. Phys. Chem.* **1962**, *66*, 561-562.
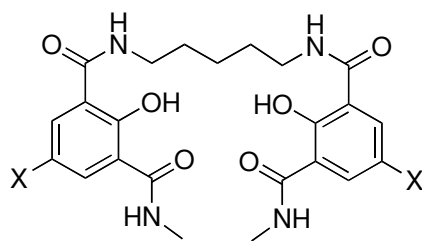
Figure 1. Structure of 5LI-IAM-X ligands (X = H, CH$_3$, (C=O)NHCH$_3$, SO$_3^-$, NO$_2$, OCH$_3$, F, Cl, Br)
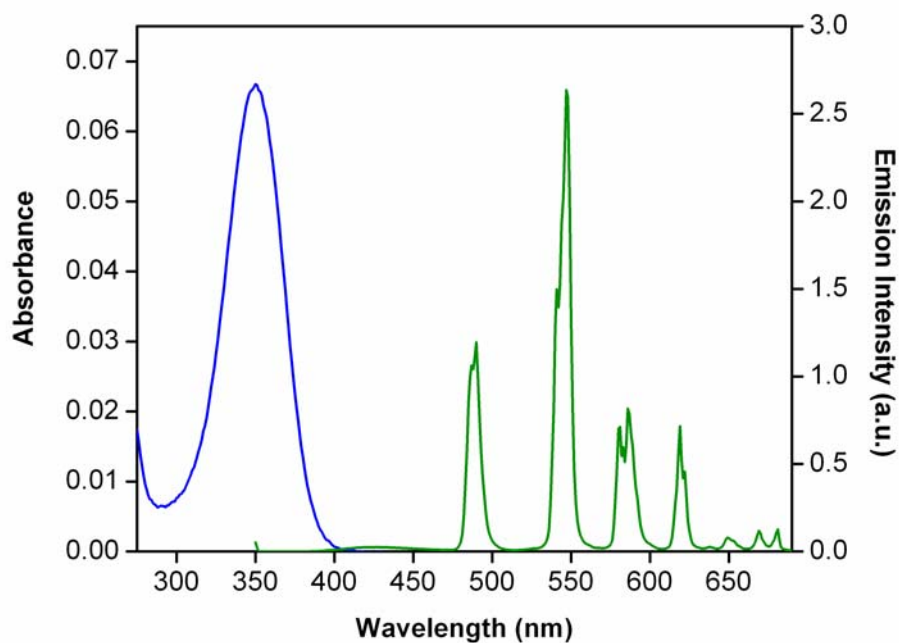
Figure 2. Absorption (blue) and emission (green) spectra of **Tb-Cl** (λ_{ex} = 350 nm). Absorption and emission spectra for the entire IAM-X series can be found in the *Supporting Information* (Figures S1-S8).
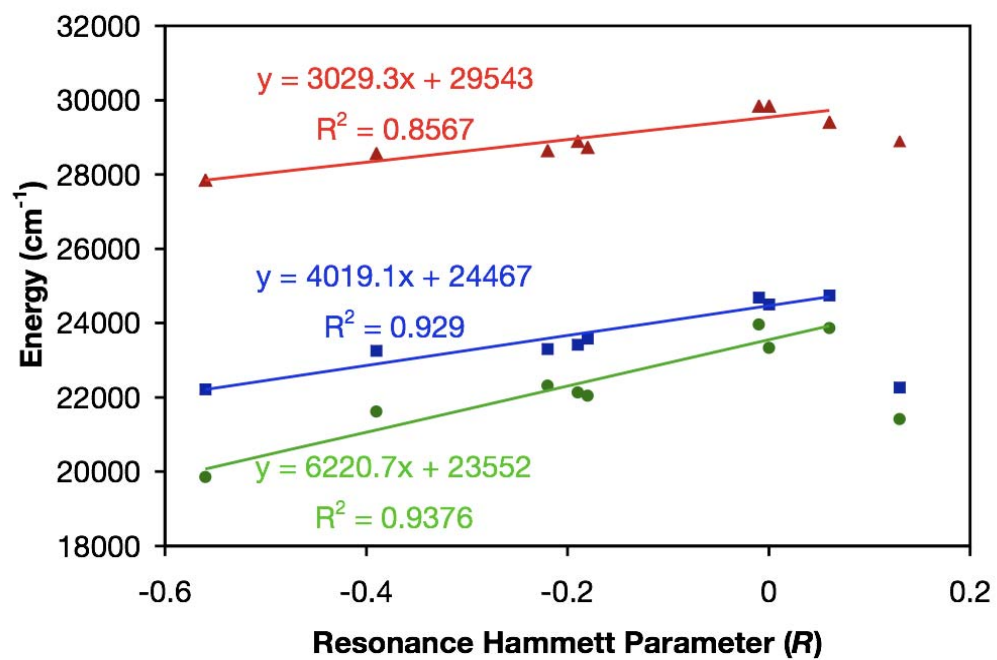
Figure 3. Linear relationships between ligand absorption maxima ( ), fluorescence maxima (¼), and triplet energies (μ) and the resonance component of the Hammett parameter of the substituents (***R***)
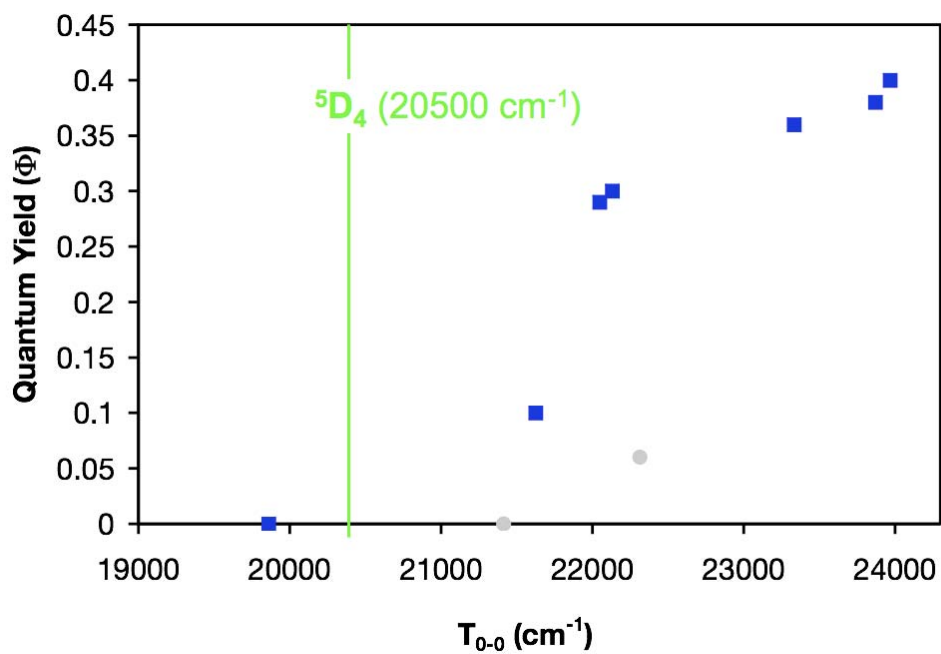
Figure 4. Relationship between the ligand triplet energies (T_{0-0}) and the quantum yields (Φ) of the corresponding Tb(III) complexes. **Tb-NO$_2$** and **Tb-Br**, which experience quenching due to an ILCT state and possible heavy-atom effects, respectively, are shown as μ.
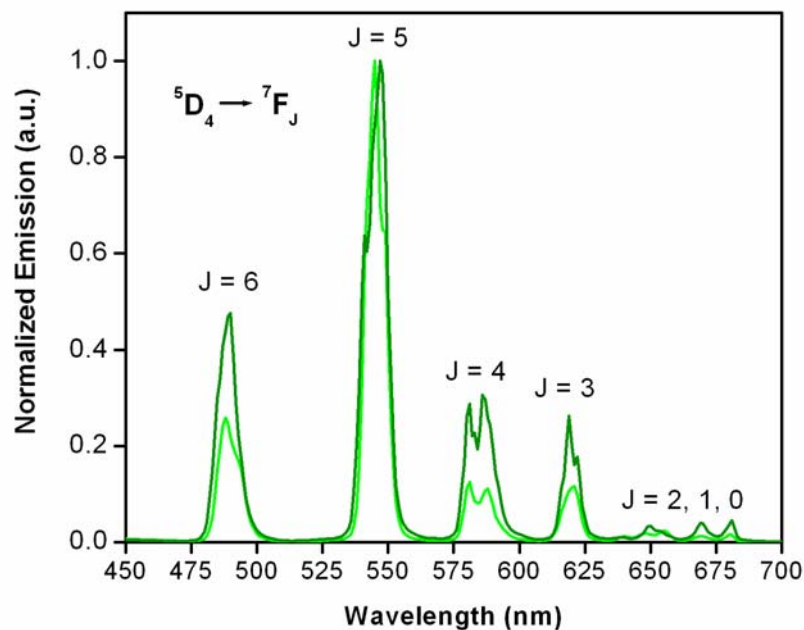
Figure 5. Emission spectra of **Tb-H** (**10f**) (dark green, λ_{ex} = 335 nm) and **Tb-SO$_3^-$** (**10i**) (light green, λ_{ex} = 340 nm) normalized to the intensity of the $^5D_4 \rightarrow {}^7F_5$ transition (C = 10^{-5} M, 0.1 M TRIS, pH 7.4, 0.2% DMSO).
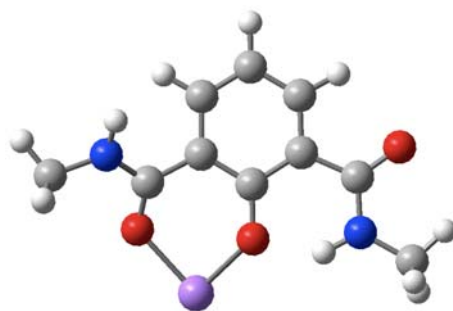
Figure 6. Representative TD-DFT input structure. The ligand is approximated as a single bidentate binding unit and the Tb(III) is replaced with Na$^+$ (purple).
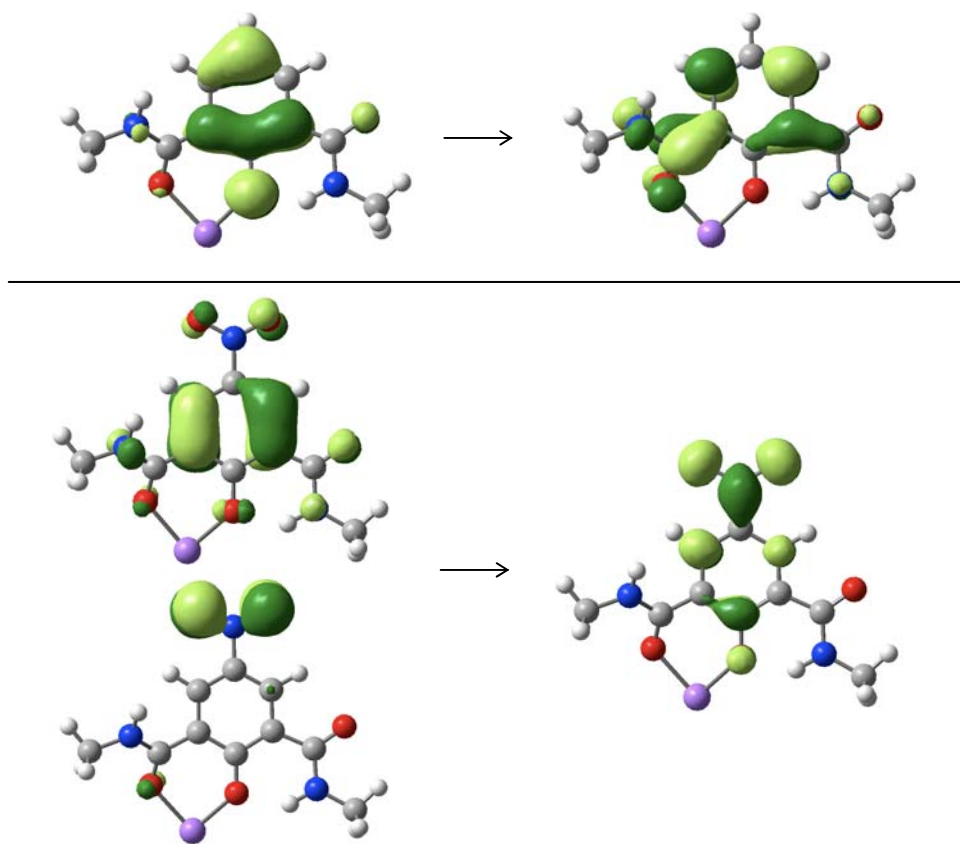
Figure 7. Representative molecular orbitals showing $\pi-\pi^*$ $S_0 \rightarrow T_1$ transition for IAM-H (top) and ILCT $S_0 \rightarrow T_1$ transition for IAM-NO$_2$ (bottom).

Scheme 1. Synthesis of 5LI-IAM-X ligand series

1a: X = Cl
1b: X = Br

2a: X = Cl, R = CH$_3$
2b: X = Br, R = CH$_3$

3c: X = F
3d: X = OCH$_3$

4c: X = F
4d: X = OCH$_3$
4e: X = CH$_3$

5c: X = F, R = Bn
5d: X = OCH$_3$, R = Bn
5e: X = CH$_3$, R = CH$_3$

6a: X = Cl, R = CH$_3$
6b: X = Br, R = CH$_3$
6c: X = F, R = Bn
6d: X = OCH$_3$ R = Bn
6e: X = CH$_3$, R = CH$_3$
6f: X = H, R = CH$_3$
6g: X = NO$_2$, R = CH$_3$

viii

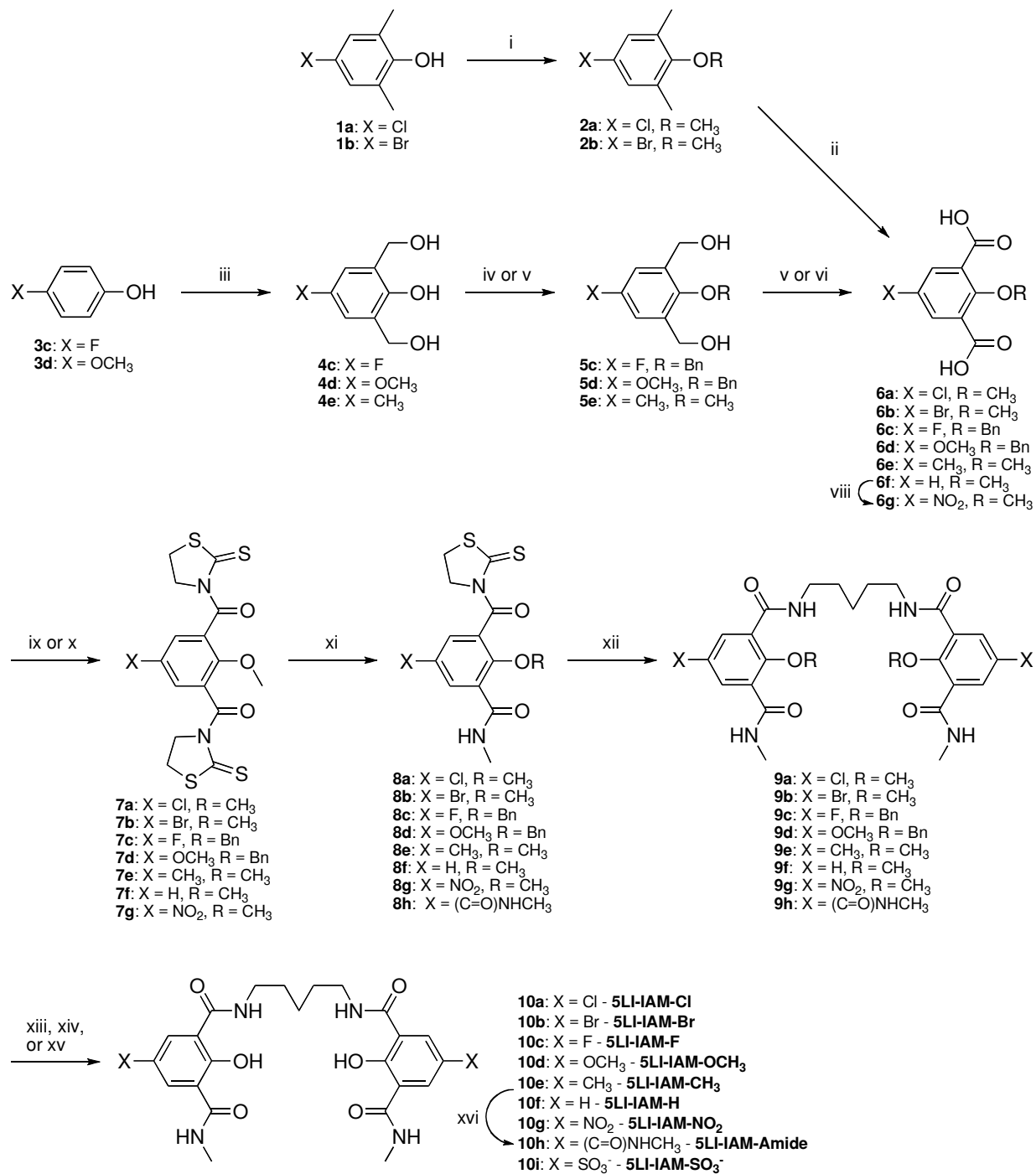7a: X = Cl, R = CH$_3$
7b: X = Br, R = CH$_3$
7c: X = F, R = Bn
7d: X = OCH$_3$ R = Bn
7e: X = CH$_3$, R = CH$_3$
7f: X = H, R = CH$_3$
7g: X = NO$_2$, R = CH$_3$

8a: X = Cl, R = CH$_3$
8b: X = Br, R = CH$_3$
8c: X = F, R = Bn
8d: X = OCH$_3$ R = Bn
8e: X = CH$_3$, R = CH$_3$
8f: X = H, R = CH$_3$
8g: X = NO$_2$, R = CH$_3$
8h: X = (C=O)NHCH$_3$

9a: X = Cl, R = CH$_3$
9b: X = Br, R = CH$_3$
9c: X = F, R = Bn
9d: X = OCH$_3$ R = Bn
9e: X = CH$_3$, R = CH$_3$
9f: X = H, R = CH$_3$
9g: X = NO$_2$, R = CH$_3$
9h: X = (C=O)NHCH$_3$

10a: X = Cl - **5LI-IAM-Cl**
10b: X = Br - **5LI-IAM-Br**
10c: X = F - **5LI-IAM-F**
10d: X = OCH$_3$ - **5LI-IAM-OCH$_3$**
10e: X = CH$_3$ - **5LI-IAM-CH$_3$**
10f: X = H - **5LI-IAM-H**
10g: X = NO$_2$ - **5LI-IAM-NO$_2$**
10h: X = (C=O)NHCH$_3$ - **5LI-IAM-Amide**
10i: X = SO$_3^-$ - **5LI-IAM-SO$_3^-$**

Reagents and conditions: (i) DMS, K$_2$CO$_3$, acetone, 56 ^{o}C; (ii) KMnO$_4$, KOH, H$_2$O, 100 ^{o}C; (iii) paraformaldehyde, NaOH, H$_2$O, 30 ^{o}C; (iv) benzyl chloride, K$_2$CO$_3$, DMF, 75 ^{o}C; (v) DMS, NaOH, H$_2$O, 25°C; (vi) CrO$_3$/H$_2$SO$_4$, acetone, 25 ^{o}C; (vii) KMnO$_4$, KOH, H$_2$O, 0 ^{o}C; (viii) 1:2 HNO$_2$: H$_2$SO$_4$, 0 ^{o}C; (ix) 1. thionyl chloride, dioxane, 100 ^{o}C 2. 2-mercaptothiazoline, NEt$_3$, CH$_2$Cl$_2$, -78 – 25 ^{o}C; (x) 1. oxalyl chloride, benzene, 50 ^{o}C 2. 2-mercaptothiazoline, NEt$_3$, CH$_2$Cl$_2$, 0 – 25 ^{o}C; (xi) CH$_3$NH$_2$, MeOH, CH$_2$Cl$_2$; (xii) 1,5-diaminopentane, CH$_2$Cl$_2$; (xiii) BBr$_3$, CH$_2$Cl$_2$, -78 – 25 ^{o}C; (xiv) 1:1 HOAc: HCl; (xv) Pd/C, HOAc, MeOH, H$_2$; (xvi) H$_2$SO$_4$.

Table 1. Summary of photophysical data for Tb(III)-5LI-IAM-X complexes ($C = 10^{-5}$ M, 0.1 M TRIS buffer pH = 7.4 (0.2% DMSO, $\lambda_{exc} = \lambda_{max}{}^{ab}$).

		$\lambda_{max}{}^{ab}$	ε	$\lambda_{max}{}^{fl}$	$T_{0-0}{}^{a}$	τ (ms) @ RT			τ (ms) @ 77K^{c}		
Ligand	X	(nm)	($M^{-1}cm^{-1}$)	(nm)	(cm^{-1})	H_2O	D_2O	q^{b}	H_2O	D_2O	Φ^{d}
10h	Amide	335	19100	405	23970	2.22	2.49	-0.1	2.17	2.57	0.40
10i	SO_3^-	340	24700	404	23870	1.23	1.42	0.2	1.12	1.22	0.38
10f	H	335	25100	408	23330	2.52	2.81	-0.1	2.46	3.11	0.36
10b	Br	349	20100	429	22310	0.943	1.18	n/a	2.28	2.87	0.06
10a	Cl	346	22100	427	22130	1.98	2.15	-0.1	2.39	2.89	0.30
10e	CH_3	348	22200	424	22050	2.04	2.31	0	2.57	3.15	0.29
10c	F	350	26200	430	21630	0.651	0.847	n/a	2.58	3.17	0.10
10g	NO_2	346	54400	449	21410	–	–	–	1.56	1.62	0
10d	OCH_3	359	22500	450	19860	–	–	–	2.67	3.22	0

[a] T_{0-0} values obtained by deconvolution of emission spectra of Gd(III) complexes (77K, 1:4 MeOH:EtOH) to determine 0-0 vibrational transition energy. [b] Calculated from room-temperature lifetime values using $q = 5 \times (1/\tau_{H2O} - 1/\tau_{D2O} - 0.06)$.[44] [c] Samples contained 10% (v/v) glycerol. [d] Error ~10% based on duplicate measurements.

Table 2. Summary of calculated singlet ($S_1{}^{calc}$) and triplet ($T_1{}^{calc}$) energies compared to experimental absorption maxima ($\lambda_{max}{}^{ab}$) and T_{0-0} energies.

	$\lambda_{max}{}^{ab}$	$S_1{}^{calc}$	T_{0-0}	$T_1{}^{calc}$
X	(nm)	(nm)	(nm)	(nm)
Amide	335	339	417	421
SO_3^- [a]	340	339	419	421
H	335	342	429	430
Br	349	355	448	454
CH_3	346	353	454	452
Cl	348	351	452	451
F	350	354	462	466
NO_2	346	354	467	498
OCH_3	359	383	504	514

[a] Input structure contained an additional Na^+ counter-ion to balance the charge.

SYNOPSIS TOC: A series of nine para-substituted antenna ligands have been prepared to study the effects of ligand substitution on Tb(III) emission in an effort to develop a predictive model of the photophysical behavior of antenna chromophores and their resulting Tb(III) complexes. Emission spectra show that the ligand singlet and triplet energies increase linearly with the resonance Hammett parameter (R) of the substituent and that the quantum yields of the Tb(III) complexes increase with the ligand triplet energies; TD-DFT calculations performed on simplified Na^+ analogs of the Tb(III) reproduce experimental ligand triplet energies within ~5%. Together, the experimental and computational results serve as a predictive tool that can be used to guide antenna ligand design.